CATALYTIC PROPERTIES OF MOLYBDENUM NITRIDE IN HYDROGENATION OF QUINOLINE

By

BYEONG IL NOH

Bachelor of Science

in Chemical Engineering

Hanyang University

Seoul, Korea

1984

Submitted to the Faculty of the
Graduate College of the
Oklahoma State University
in partial fulfillment of
the requirements for
the degree of
MASTER OF SCIENCE
December, 1988

CATALYTIC PROPERTIES OF MOLYBDENUM NITRIDE IN HYDROGENATION OF QUINOLINE

Thesis Approved:

Thesis Adviser

Dean of the Graduate College

ABSTRACT

Improved methods for hydrodenitrogenation of fuels will become of greater importance in the future as it becomes necessary to rely increasingly on processing of lower grade petroleum and liquids derived from coal and oil shale. Model compound studies of various heterocyclic nitrogen compounds have shown that hydrodenitrogenation proceeds via saturation of the heterocyclic ring, followed by hydrogenolysis of C-N bonds. These reactions consume more hydrogen than hydrodesulfurization reactions which do not need any ring saturation over the same catalysts.

In this study, the performance of an unsupported molybdenum nitride powder has been investigated for the hydrogenation of quinoline in a batch reactor at 10.4 MPa (1500 psig) and 270 to 330 °C. 3-5 g of the catalyst was added to a mixture of 10 wt.% quinoline in n-hexadecane and the products were compared with those from noncatalytic reactions. The unique hydrocarbon product of both catalytic and noncatalytic reactions was identified as 1,2,3,4 - tetrahydroquinoline. This confirmed the specific selectivity of molybdenum nitride catalyst and that only the pyridine side of quinoline adsorbed on the surface of catalyst. However, it was found that the catalyst has very low activity at the

reaction conditions, compared with that of a presulfided commercial HDN catalyst. The kinetics of hydrogenation of quinoline have been studied by the first order reversible reaction model and the rate constants and the activation energies were calculated. The rate constants at 270, 300, and 330 °C are 0.00262, 0.0124, 0.0394 (1 / g cat. hr), respectively which result in an activation energy of 165 kJ/mol (39.4 kcal/mol). These rate constants were compared with those of the reaction over sulfided catalysts in order to evaluate the catalytic activity of the molybdenum nitride. Catalyst characterization studies showed that the physical structure of the catalyst changed during the reaction, resulting in an increase in the surface area.

ACKNOWLEDGMENTS

I wish to express sincere appreciation to my major advisor, Dr. Mayis Seapan for his intelligent guidance, inspiration and invaluable aid throughout my graduate program. Many thanks also go to Dr. A. H. Johannes and Dr. G. L. Foutch for serving on my graduate committee. Their suggestions and support were very helpful throughout the study.

A note of thanks is given to Yung N. Lee, Randy Smerkjel, and Danise Rex for their help in conducting the experiments and analysis. Without their involvement this study would not have been possible.

My parents encouraged and supported me all the way and helped me keep my goal constantly in sight. Thanks go to them for their undivided time in the final stages of the project. My wife Hyogeun provided moral support and was a real believer in my abilities. Without friends like Sungsun, Inchul, Hyungeun, Jungil, and Juchun, this endeavor would not have been as educational and stimulating. I extend a sincere thank-you to all of these people.

Finally, I would like to express my gratitude to the School of Chemical Engineering for supporting me in this project and during my coursework.

TABLE OF CONTENTS

Chapter Page

LIST OF TABLES

LIST OF FIGURES

Figure Page

NOMENCLATURES

HDN	Hydrodenitrogenation
HDS	Hydrodesulfurization
Py-THQ	1,2,3,4 - tetrahydroquinoline
Bz-THQ	5,6,7,8 - tetrahydroquinoline
DHQ	Decahydroquinoline
PCH	Propylcyclohexane
OPA	o-Propylaniline
PBZ	Propylbenzene
$k_{1,2}$	Forward or backward reaction rate constants of the first order homogeneous reversible reaction, 1/hr
k'	Pseudo-first order rate constant, $k_1 * P_{H2}^2$, 1/hr, 1/(g cat. hr), or 1/(surface area * hr)
K_j	Adsorption equilibrium constant in the reaction j
r	Reaction rate, mol/(g cat.* hr* vol. of reactor)
C_i	Concentration of component i, mol/vol. of reactor
P_{H2}	Partial pressure of hydrogen, psia
X_A	Fractional conversion of A
X_{Ae}	Fractional conversion of A at equilibrium state
t	Reaction time, hr
T	Temperature, ^oC
l,m	Adsorption sites for quinoline and hydrogen

CHAPTER I

INTRODUCTION

The importance of hydrotreatment processes for the removal of heteroatoms from liquid fossil fuels is increasing, owing to both economic and environmental constraints. In response to the recent decline in conventional energy sources, interest in the upgrading of heavy residual fractions and the use of petroleum alternatives such as shale oil, coal liquids, or tar sand oil has refocused attention on both hydrodenitrogenation (HDN) and hydrodesulfurization (HDS) processes.

The nitrogen-containing compounds in the synthetic oils are primarily of condensed, heterocyclic form such as indole, carbazole, quinoline, and acridine. These compounds interfere with other catalytic reactions such as catalytic cracking, lead to poor color and instability of products, and in the concentrations existing in unprocessed fuels may produce unacceptably high levels of NO_x in combustion gases. Among the various types of these nitrogen compounds, quinoline, which possesses a benzene ring and a pyridine ring is a good model compound for characterization of HDN reactions because of the assumption that its behavior in hydrotreating is similar to those of most nitrogen heterocycles contained

in the synthetic oils.

HDN has not received as much attention as has HDS because sulfur compounds have historically been of primary concern. However, with the increasing need for more effective HDN processes, HDN is being recognized as an important part of heavy fuel processing. HDN is the more difficult and more demanding of the two hydrotreating reactions, and requires more sever reaction conditions than does HDS (Satterfield, Modell, and Mayer, 1975). Most of the studies of the HDN reactions use a supported transition metal such as Mo or W oxide with either Co or Ni promoters as a catalyst. Sulfidation of these catalysts, either by H_2S or by an organic sulfur compound, accelerates the rate of the catalytic HDN and promotes the rate of reduction of the nitrogen-containing aromatic ring (Satterfield, Modell, and Mayer, 1975 ; Rollman, 1977). However, the fundamental basis for the origin of the catalytic activity of the sulfided catalysts remains unclear.

It has been found that denitrogenation of the unsaturated heterocyclic nitrogen compounds over either a sulfided or unsulfided catalyst requires more hydrogen consumption than desulfurization. Denitrogenation needs the complete saturation of the rings prior to the breakage of the carbon-nitrogen bond, whereas the ring saturation is not required for desulfurization over the same catalysts (Sonnemans and Mars, 1973). In order for the synthetic oils to become competitive energy sources, catalysts and operating

procedures which can remove nitrogen with reduced cost are desired. One of those possible methods can be the use of a nitrided transition metal catalyst. The idea to use a nitride catalyst for HDN originates from the use of sulfided catalysts for HDS, with the hope that nitrogen atoms will be removed without saturation of the aromatic rings, reducing the consumption of expensive hydrogen. It was expected at the beginning of this project that the nitride would be a good HDN catalyst. However, this work showed that it does not have the capability to break the nitrogen-carbon bond in heterocyclic ring at the reaction conditions, and it can only hydrogenate the pyridine ring.

This project is undertaken to study the catalytic properties of molybdenum nitride in the hydrogenation of quinoline and to compare its catalytic activity with that of sulfided commercial catalysts and finally to model the kinetics of hydrogenation of quinoline.

CHAPTER II

LITERATURE REVIEW

An excellent review of the literature of the HDN of quinoline has been compiled previously (El-Bishtawi, 1986 ; Lee, 1988) ; hence, only the important aspects of HDN reactions related to the work done in this thesis are reviewed in this chapter. Also reviewed are the literature pertaining to the transition metal nitrides.

Hydrogenation of Quinoline

Catalytic hydrogenation of quinoline in the first step produces 1, 2, 3 ,4 - tetrahydroquinoline (Py-THQ), 5, 6, 7, 8 - tetrahydroquinoline (Bz-THQ), and cis- and trans-decahydroquinoline (DHQ). Under severe reaction conditions, the hydrogenation reaction leads to breakage of the ring system of quinoline, producing ammonia, amines, and hydrocarbons. Figure 1 shows the steps that are currently believed to be significant in the overall quinoline HDN reaction network.

The earliest reports of catalytic hydrogenation of quinoline, producing decahydroquinoline, were by Ipatiev (1908) over a nickel oxide catalyst and by Sabatier and Murat (1914) over a nickel catalyst. The easiest

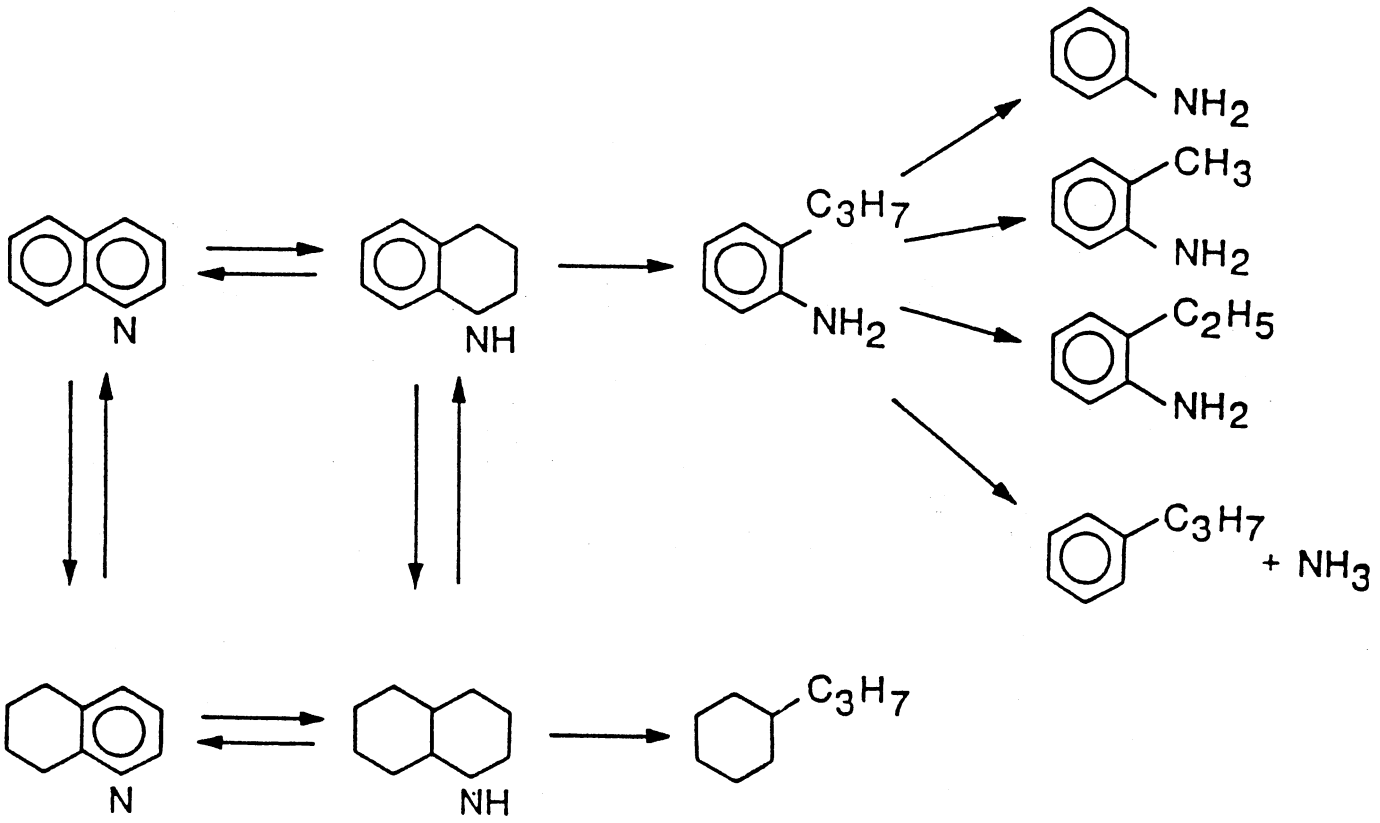

Figure 1. Reaction Network for Quinoline HDN at 357-390 C, 8.2 MPa, HDS-9A Catalyst (El-Bishtawi, 1986)

hydrogenation product to obtain is Py-THQ. Wedekind and Maiser(1928), Braun, Petzold, and Seeman(1922), and Palfray (1940) reported quantitative yields of Py-THQ with nickel at 200 °C and 30 atm. Lower but still good yields have been reported when using tungsten-nickel sulfide 8376 (Eru, et al., 1963), tungsten disulfide-nickel oxide-alumina (25 : 5 : 70) and tungsten disulfide-alumina (Weiser, 1973). Other reports of the preparation of Py-THQ concern with the use of calcium metal and hydrogen (Berhstrom and Carson, 1941) and aluminum-nickel catalyst in a flow apparatus under pressure, giving mixed tetra- and deca-hydroquinolines (Ponomarev and Dyukareva, 1973).

A number of studies on the destructive hydrogenation of quinoline have been performed. High-pressure and high-temperature hydrogenation over cobalt sulfide by Roberti (1932), over molybdenum sulfide by Shono et al. (1963), or over various mixtures of cobalt, molybdenum, nickel, and alumina by Aboul-Gheit and Abdou (1973), and Svajgl (1974) were reported to give ammonia and hydrocarbon mixtures. These procedures have been used to denitrogenate paraffins contaminated with quinoline. Sultanov et al. (1965) reported the presence of the two tetrahydroquinolines, trans-decahydroquinoline, 2- and 3-methylindole, indene and octahydroindene, anilines, benzene, toluene, ethylbenzene, n-propylbenzene, hexane, and the corresponding cyclohexanes in the product of quinoline hydrogenation over molybdenum sulfide at 360 °C, 100atm.

Quinoline is generally accepted as being more reactive towards hydrogenation than benzene ; competitive experiments showed pyridine and quinoline to be approximately equally reactive (Diworky and Adkins, 1931). A kinetic study showed that the hydrogenation of quinoline with platinum oxide as a catalyst was first order in hydrogen and zero order in the quinoline concentration (Nakhmanovich and Kalechits, 1964).

Flinn et al. (1963) studied the HDN of quinoline over a presulfided Ni-W/alumina in a high purity paraffin oil and reported that the reaction involves ring hydrogenation which is the rate-controlling step, followed by nitrogen removal.

Doelman and Vulgter (1963), performing their experiments in a fixed bed reactor using a Co-Mo/alumina catalyst, found that around 300 °C, some 90 % of quinoline is hydrogenated resulting in Py-THQ. The quantity of Py-THQ decreases with increasing temperature and above 350 °C, Bz-THQ is formed. The formation of Bz-THQ is favored by higher temperatures and also by lower feed rate. They reported that the amount of Py-THQ present in the reaction products decreases more rapidly with increasing temperature than that of Bz-THQ. This means that the carbon-nitrogen bond of the saturated pyridine ring is broken to give rise to various amines much more easily than that of the unsaturated pyridine ring. Therefore, Bz-THQ is more stable than Py-THQ.

Shih et al. (1977) also studied quinoline HDN using

presulfided HDS-9A catalyst and a highly paraffinic white oil as a solvent at 3.4 MPa and 342 °C. They added an amount of CS_2 equivalent to 0.05 wt.% of the carrier oil to the catalyst and quinoline to maintain the sulfided state of the catalyst during the reactions. They concluded that HDN of quinoline involves hydrogenation and hydrogenolysis of the resulting piperidine ring and subsequent deamination. Hydrogenation takes place through two routes, the pyridine-ring saturation route resulting in the formation of Py-THQ, and the benzenoid-ring saturation route resulting in the formation of Bz-THQ. By subsequent hydrogenation, these two routes produce DHQ as another reaction intermediate of HDN of quinoline. They suggested a reaction network in which nitrogen removal occured mainly through the hydrogenolysis of DHQ and reported that the hydrogenation reactions were first order with respect to nitrogen content, while they are second order in hydrogen. Also reported are the rate constants and estimated activation energies for each step of reaction in quinoline HDN network. It was found that the reaction between quinoline and Py-THQ attains the equilibrium state very fast and the other reaction steps are irreversible.

Satterfield et al. (1978) studied the intermediate reactions in the HDN of quinoline in the vapor phase in a continuous-flow microreactor at 3.55 MPa and 7.0 MPa and at temperatures of 230 to 420 °C with a sulfided Ni-Mo/alumina catalyst. They reported the heat of reaction between

quinoline and Py-THQ and the equilibrium constant. The average value of the heat of reaction is 32 ± 1.2 kcal/mol. It was concluded that quinoline and Py-THQ are in thermodynamic equilibrium under essentially all reaction conditions of interest. Thus at increased temperatures and lower hydrogen pressures the equilibrium shifts back toward quinoline. The quinoline is then converted to Bz-THQ and subsequently to DHQ and its products.

Cocchetto and Satterfield (1976) estimated the thermodynamic equilibrium between quinoline and Py-THQ in conjunction with theoretical estimations of the equilibria of various steps in HDN reactions of a variety of heterocyclic nitrogen compound. From a plot of equilibrium constant versus inverse time, the heat of reaction was calculated to be 31.3 kcal/mol by the Van't Hoff relationship. They also summarized the postulated HDN mechanisms of representative heterocyclic nitrogen compounds.

Bhinde (1979) investigated interaction effects of simultaneous HDN, HDS, and hydrogenation in a batch autoclave under commercial reaction conditions. He found that the rate of total nitrogen removal, the disappearance of the lumped group of quinoline, Py-THQ and other individual reactions follow pseudo-first order kinetics, and that quinoline and Py-THQ rapidly attain thermodynamic equilibrium. He also found that quinoline molecules are adsorbed on one type of catalytic site and hydrogen is adsorbed on a different site.

Cocchetto et al. (1981) demonstrated that the reactions among quinoline and its three hydrogenated derivatives are reversible. They used a continuous-flow microreactor and calculated the equilibrium constants of the various steps believed to be of significance in the quinoline HDN reaction network. Only equilibrium constants at 330 °C for the reactions between quinoline and Py-THQ could not be estimated accurately from the experimental data because of severe kinetic limitations at this relatively low temperature. It was concluded that the HDN reaction pathways of minimum hydrogen consumption are not thermodynamically favored under industrial conditions, so the burden of selectively hydrogenating only the heteroring is placed solely on the catalyst. However, present commercial hydrotreating catalysts have been shown to exhibit little selectivity for HDN reaction pathways of minimum hydrogen consumption (Shih et al., 1977 ; Satterfield and Cocchetto, 1981).

Satterfield et al. (1981) studied reaction network and kinetics of the HDN of quinoline in the vapor phase, using a continuous-flow microreactor at 3.55 and 7.0 MPa, 330 to 420 °C over presulfided Ni-Mo/alumina catalysts. They reported that the unexpected departure of the Py-THQ/quinoline product ratio from equilibrium at longer contact times can be interpreted in terms of competitive adsorption effects, postulating that quinoline is more weakly adsorbed on the surface of the catalyst than Py-THQ. Adsorption of nitrogen compounds is believed to occur through the interaction of

the basic nitrogen group with acidic sites on the catalyst. Therefore, more basic nitrogen compounds such as Py-THQ and DHQ are likely to be more strongly adsorbed than quinoline. Thus, after initial equilibrium with Py-THQ, quinoline was prevented from adsorbing and reacting on the catalyst until the concentration of Py-THQ had decreased significantly.

Satterfield and Gültekin (1981) studied the effect of H_2S on the catalytic HDN of quinoline in the vapor phase and reported that the presence of H_2S has a slightly inhibiting effect on the intermediate hydrogenation steps but a marked accelerating effect on the overall HDN rate. Rate constants and activation energies for a set of standard conditions are also reported for most of the intermediate reaction steps, in the presence and absence of H_2S.

More recently, Yang and Satterfield (1983) reported that H_2S has little effect on the activation energies of the hydrogenation and dehydrogenation reactions in the overall reaction network of the quinoline HDN, but it significantly reduces those for the hydrogenolysis reactions. These effects of H_2S can be explained by the competitive adsorption of H_2S and substrate on the catalytic centers ; H_2S adsorbed on these centers would act as a cocatalyst for carbon-nitrogen bond cleavage. Satterfield and Carter (1981) reported that this marked enhancing effect of H_2S on the HDN of quinoline reaction rate is not significantly affected by the presence of water vapor.

Fish et al. (1984) investigated the selective reduction

of polynuclear heteroaromatic nitrogen compounds such as quinoline, acridine, and so on over chlorotris (triphenylphosphine) rhodium, $(Ph_3P)_3RhCl$ under rather mild hydrogenation conditions and showed that the reduction of the carbon-nitrogen double bond is the initial product of hydrogen transfer from rhodium to the complex substrate, followed by a reversible dehydrogenation step that must have a comparable rate to the stereospecific reduction of the 3, 4-double bond in compounds such as quinoline. It was also observed that both steric and electronic effects control the initial hydrogenation rates of substrates in the presence of compounds that can competitively bind to the rhodium metal center as well as those that enhance initial rates of hydrogenation.

Glola and Lee (1986) studied the effect of hydrogen pressure on catalytic HDN of quinoline in a stirred batch reactor at constant temperature of 350 ^{o}C and in the presence of a presulfided catalyst (Ni-Mo/alumina). The hydrogen pressure, kept constant during each run, was varied in the range of 10.5 to 151.6 bar. They reported that a necessary condition for the elimination of the nitrogen atom is that the hydrogenation of the rings containing nitrogen be completed first. Thus both the hydrogen consumption and the overall rate of denitrogenation increase with pressure. The reaction network together with the kinetic constants of the reactions involved was identified from a statistical analysis of their experimental results at each pressure. It was

concluded that hydrogen adsorption sites are different from those for organic compounds and that quinoline and Py-THQ are adsorbed preferentially, as compared to the other organic compounds. Finally, most hydrogenation and dehydrogenation reaction rates obey Langmuir-Hinshelwood theory, showing the dependence on hydrogen pressure.

El-Bishtawi (1986) studied the HDN of quinoline in an autoclave batch reactor over a commercial NiMo/alumina catalyst (American Cyanamid HDS-9A) under the experimental conditions of 357 - 390 °C and 10.4 MPa. The formation of Py-THQ decreases and the formation of Bz-THQ increases with increasing reaction temperature. Futhermore, temperature does not affect the equilibrium conversion of quinoline, significantly. It was found that the model derived by assuming different adsorption sites for hydrogen and nitrogen compounds yielded the best fit of the experimental data. He proposed a reaction network in which once OPA is formed from Py-THQ, only various aniline and benzene compounds are formed and propylcyclohexane (PCH) is exclusively formed from DHQ.

Curtis and Cahela (1987) investigated the effectiveness of unsupported, precipitated transition metal sulfides, RuS_2 and MoS_2, as HDN catalysts in both a quinoline system and a coal liquefaction system. These transition metal sulfides possessed HDN selectivity in the quinoline system and rivaled the commercial hydrotreating catalysts in activity ; RuS_2 was comparable to Ni-Mo/alumina and MoS_2 to

Co-Mo/alumina. However, RuS_2 was not as severely poisoned by quinoline as NiMo/alumina. Both RuS_2 and MoS_2 achieved upgrading in coal liquefaction reactions and the higher surface area Ni-Mo/alumina showed considerably more nitrogen removal.

Most recently, Lee (1988) studied the kinetics of quinoline HDN reactions by using each intermediate compound in reaction network as the feed in a gradientless reactor with Berty type internals under the reaction conditions of 10.4 MPa and 350 °C over a Ni-Mo/alumina catalyst. The primary route for the removal of nitrogen atom from quinoline was the formation of Py-THQ. This was followed by further hydrogenation to DHQ, and breakage of the nitrogen containing ring of DHQ to form PCH. The rate limiting step was the processing of Py-THQ. Through the adsorption study, he found that Py-THQ had the strongest adsorptivity among all of the intermediate compounds, whereas DHQ had the lowest value and that there was no correlation between the adsorption constant and the compound basicity. He reported the adsorption constants of all of the intermediate compounds and the rate constants of each step in the HDN of quinoline, suggesting a slightly different reaction network for quinoline HDN from the previous investigators. His reaction network shows that the step between Py-THQ and DHQ can be considered to be irreversible and that PCH and propylbenzene (PBZ) can be produced from any nitrogen containing compound in the system and the step between PCH and

PBZ should not be ignored as was done in previous works.

Transition Metal Nitrides

A lot of studies have been done on the catalytic properties of transition metal nitrides for the reactions such as CO hydrogenation and C_2H_6 hydrogenolysis (Ranhotra , et al.,1986 ; Logan, et al., 1985), olefin hydrogenation (Leary, et al., 1986), methanation and Fischer-Tropsch synthesis (Saito and Anderson, 1981), ammonia synthesis (Boudart, et al., 1980 ; Volpe, et al., 1986), and CO oxidation (Yang et al., 1984). Most of these studies have focused on Mo_2N as the catalyst.

In most reactions, with the notable exception of the hydrogenation-dehydrogenation reactions, the nitrides display a low reactivity in comparison to the transition metals. However, what distinguishes the nitrides from their respective metals is their unusual selectivity patterns. No literature is available for the HDN or HDS of heterocyclic aromatic compounds containing nitrogen or sulfur over transition metal nitride as a catalyst.

What brings nitrides to the attention of the catalytic scientists is the development of a modest literature in the last decade and the demonstration that transition metal nitrides sometimes have a catalytic advantage relative to the parent transition metal (i.e., level of activity, activity maintenance, selectivity, resistance to poisoning, etc.).

Toth (1971) reviewed the properties of transition metal nitrides. According to his review, nitrides of transition metals not only have very high melting points but also have higher values of hardness. In general, the highest melting transition metals are found in group VIB of periodic table, whereas for nitrides, they are found in group IVB. This shift from right to left upon compound formation suggests interesting systematic modifications that occur in the properties of nitrides of transition metals. A crude interpretation of this trend is that the maxima are to be associated with the formation of a half filled d-shell and that to achieve this nitrogen donates two electrons to the metal. These materials render the compound resistance to attrition and sintering and make them good candidates for catalysts. Furthermore, they are usually much less expensive than the noble group VIII metals.

Levy (1977) has suggested that the high thermal stability of nitrides might have attracted the attention of the practical catalytic chemists. But he makes it clear that the significant modification of the electronic structure of the transition metal reflected in its catalytic properties continues to hold our interest.

One of the most important challenges in catalyst development is the synthesis of transition metal nitrides with high surface areas. Most studies have been done on powders of at most 5 m^2/g (Levy and Boudart, 1973). Nitrides are usually prepared by the reaction of the metal or oxide with

a nitrogen-containing gas (Toth, 1971) and temperatures of preparation are above 1000 °C. Most of the preparative procedures are designed to produce dense metallurgical materials rather than high surface area catalysts.

Volpe and Boudart (1985) have demonstrated recently that high surface area Mo_2N and W_2N powders can be prepared by temperature programmed reduction of the corresponding oxides with ammonia. They described the procedure that the face centered cubic (fcc) Mo_2N is produced by reduction of MoO_3 in NH_3 flowing at 135 m^3/min. The reduction temperature is increased from 623 to 723 °K over a 3 hours period, then from 623 to 973 °K over 2 hours period, and finally held at 973 °K for 1 hour. The final Mo_2N product consists of single crystal platelets containing pores of an average size below 30 A.

Most recently, Ranhotra et al. (1987) have studied the effects of catalyst preparation and pretreatment on the composition and structure of Mo2N (fcc). They prepared the catalysts by the same method described by Volpe and Boudart (1985) and used X-ray diffraction (XRD) and electron microscopy for structural characterization of the samples. They reported that the nitride has a high degree of crystallinity, a BET surface area of about 180 m^2/g, and pores about 17 A in diameter.

There has been considerable efforts in the past 40 years to formulate a model of the bonding of transition metal nitrides which accounts for their properties. This

effort has concentrated on two topics ; the relative importance of metal-metal (M-M) versus metal-nonmetal (M-X) interactions and direction of charge transfer between the metal and nonmetal. Oyama et al. (1981) reported that donation of electrons by the nonmetal to metal will strengthen the M-M interaction, whereas donation in the reverse direction will strengthen the M-X interaction. In spite of much of experiments and theoretical discussion, it is obvious that the question of the direction of electron transfer is still not clear. However, most authors now agree that both M-M and M-X interactions are important in the bonding, and the general concesus is that there is donation of electron from metal to nonmetal for nitrides (Levy, 1977).

Aika and Ozaki (1969) studied the synthesis of ammonia on Mo_2N at the pressures closed to atmospheric pressure and found fairly low reaction rates. They obtained a STY (site time yield) value of 0.0022 (1/ks), which is defined as the average number of product molecules produced in a catalytic bed per second per surface metal atom. They used a stoichiometric H_2 : N_2 mixture at 603 ^oK.

Boudart et al. (1980) compared the steady state activity in ammonia synthesis of various molybdenum catalysts to those of iron and ruthenium. The activity of Mo catalysts is in between that of Ru and Fe, which are generally considered as the most active metals for synthesis of ammonia and used widely in the industry. They also reported that the

composition of molybdenum surface determines the catalyst activity and selectivity and that during the reaction, oxygen and carbon in molybdenum oxycarbon catalysts are progressively replaced by nitrogen.

Most recently, Volpe and Boudart (1986) studied ammonia synthesis on three different particle sizes of Mo_2N at 1 atm pressure between 557 and 717 ^oK. They confirmed the structure sensitivity of the rate of ammonia synthesis and found that the product, ammonia, inhibited the rate at low efficiencies. Because the heat of dissociative adsorption of N_2 on Mo_2N surface (380 kJ/mol) is greater than that on iron surface (220 kJ/mol), they concluded that this inhibition resulted from higher affinity (binding energy) of hydrogen atoms for the Mo_2N surface.

Haddix et al. (1987) studied the dissociative adsorption of hydrogen on a high surface area ($120m^2/g$) γ-Mo_2N, using nuclear magnetic resonance (NMR) techniques. Based on proton NMR measurements, they concluded that hydrogen adsorbs on the surface of γ-Mo_2N in the form of rafts of localized hydrogen atoms which occupy only 10 % of the total BET surface area. They also concluded that the irreversibly held H_2 is strongly bound to the nitride surface. The occurrence of H_2 in the form of rafts of strongly bound hydrogen atoms suggests that H_2 adsorption occurs at nitrogen-deficient patches of Mo present on the nitride surface. Therefore, it is expected that the presence of nitrogen atoms on the surface of Mo should suppress the adsorption of

H_2. They finally suggested that in ammonia synthesis, the rate limiting step was the surface hydrogenation step since the adsorption of strongly bound hydrogen atoms in small rafts could limit the availability of hydrogen in surface reactions.

CHAPTER III

EXPERIMENTAL APPARATUS AND ANALYTICAL TECHNIQUES

Experimental Apparatus

Fig. 2 shows a schematic diagram of the batch reactor system used in this study. The system was designed and used by an earlier investigator at Oklahoma State University (El-Bishtawi, R. F., 1986) and some modifications were made in this project. This system is composed of the reactor and its accessories for gas feeding, venting, and sampling as well as temperature and pressure measurement and control devices.

The Reactor

This experiment was done in a 1-liter autoclave batch reactor (Autoclave Engineers, 316 SS) with internal diameter of 0.076 m (3 in.) and height of 0.229 m (9 in.). Figure 3 shows the details of the reactor internals. The reactor was equipped with a glass liner of diameter 0.0747 m and length of 0.191 m for separation of the reacting components from the metallic reactor wall. A cooling coil was employed so that water as a cooling medium could be introduced to cool the reactor system down during the reaction. The reactor

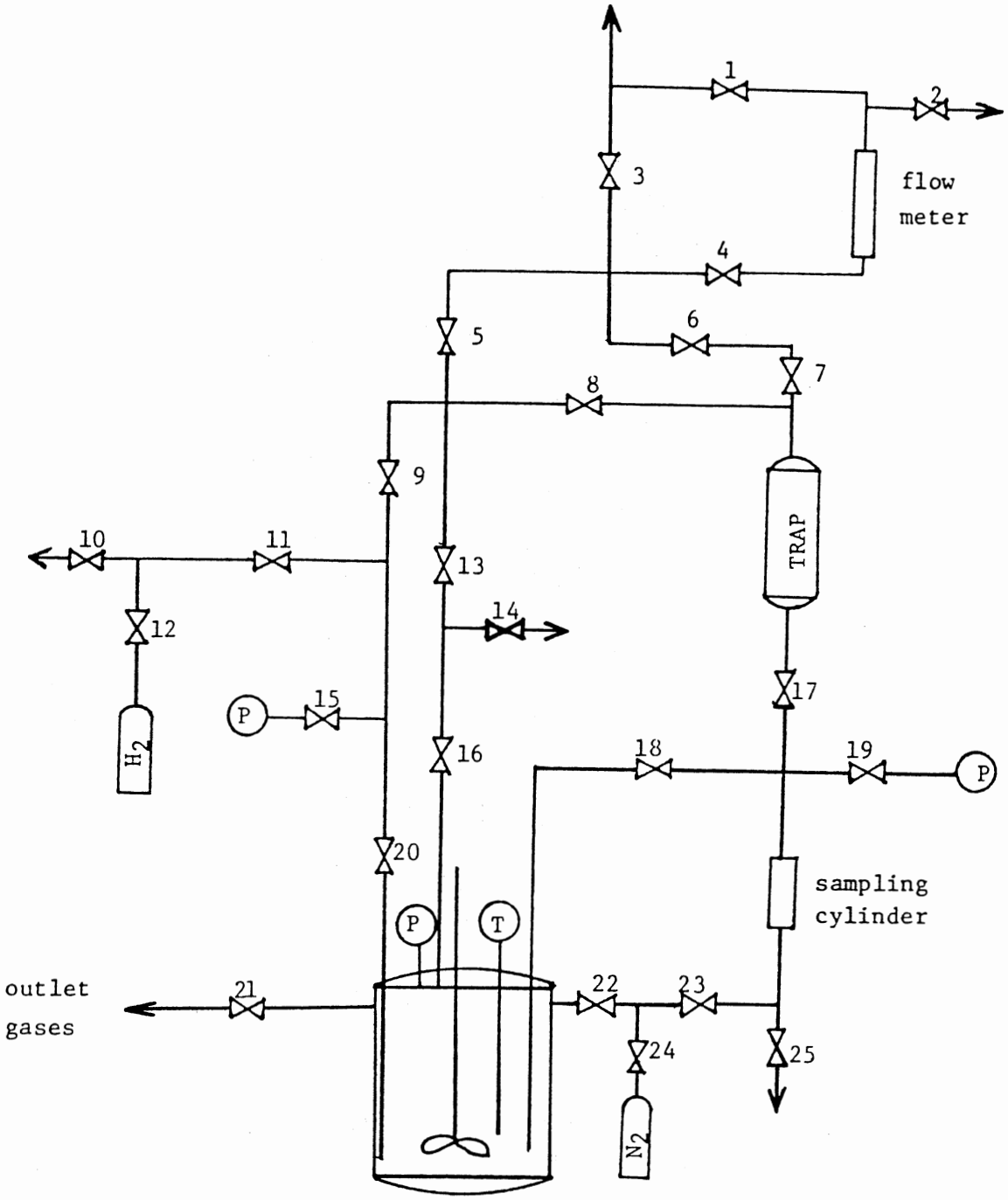

Figure 2. Schmatic Diagram of the Reactor System

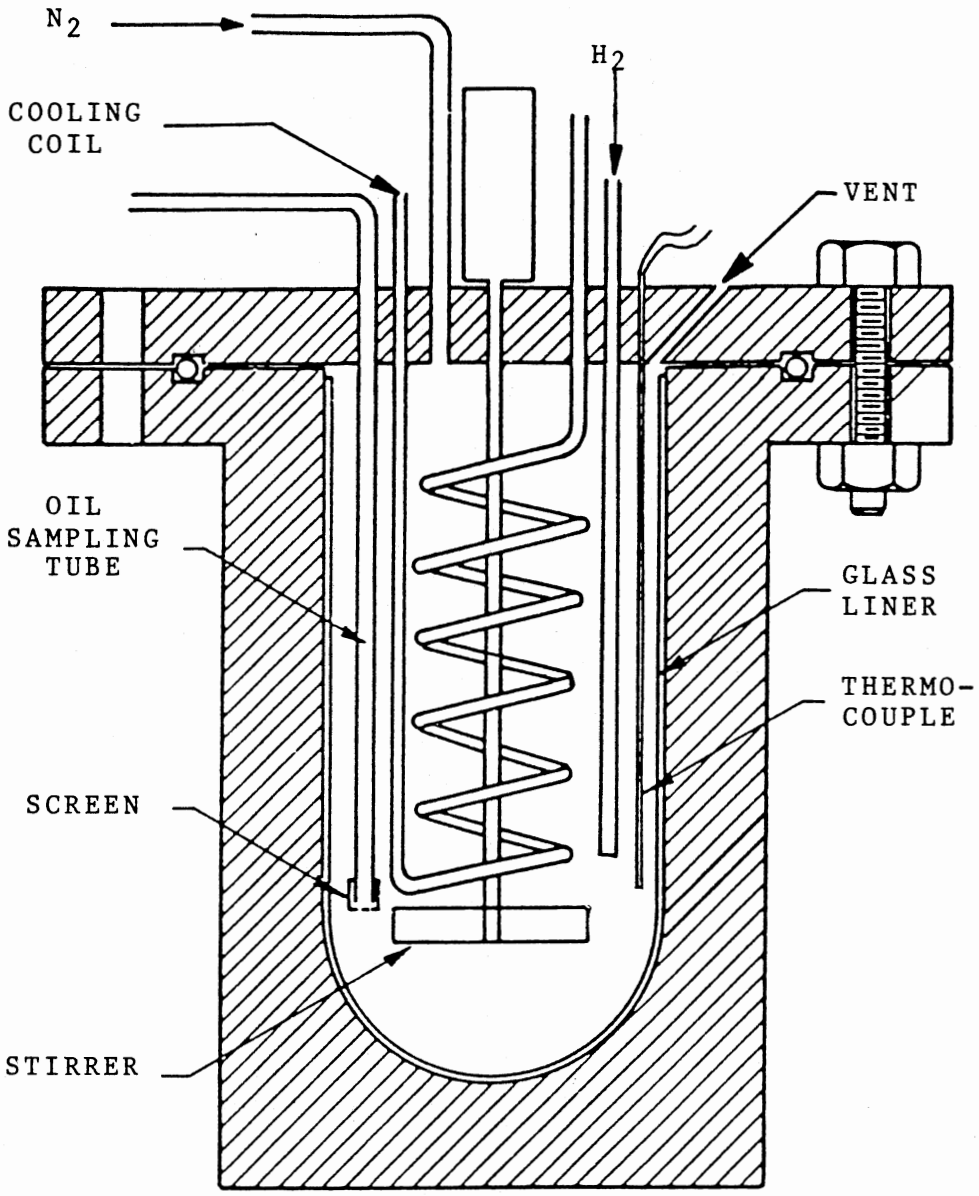

Figure 3. Schematic Diagram of Reactor Internal

was also equipped with a turbine - type agitator and two rupture discs with bursting pressures of 20.7 and 27.6 MPa (3000 and 4000 psig).

Gas Feeding

Gases including hydrogen and nitrogen were brought to the autoclave from their respective gas cylinders through appropriate valves. They entered the autoclave body through special ports. Nitrogen gas used to pressurize the reactor before heating up flowed into the top of the reactor from its cylinder through valves 24 and 22. However, hydrogen gas was introduced into the bottom of the reactor through valves 11 and 20, in order to provide good mixing with the liquid in the reactor. A regular pressure gauge with accuracy of 0.5 %, was used to monitor the reactor pressure.

Sampling

Liquid samples were drawn from the reactor through the sampling tube after the stirrer was turned off. The end of the sampling tube was located close to the bottom of the reactor in the liquid phase. A fine screen attached to this end prevented the catalyst particles from entering into the sampling tube. The other end of the tube was vented to a 30 ml sampling cylinder which was finally connected to the atmosphere through a trap. The sampling cylinder was equipped with a pressure gauge and a heating tape and was insulated. The heating system was useful especially during

winter when the liquid samples could have frozen in the sampling cylinder.

Analytical Instruments

Analytical instruments used in this project consisted of two groups, one for the analysis of liquid samples and the other for the catalyst analysis.

Liquid Analysis. The analytical tool to measure the concentration of the reaction product was a Hewlett Packard Model 5890A Gas Chromatograph (GC), equipped with a 60 m DB-1 capillary column and Thermal Conductivity Detector (TCD). A Hewlett Packard Integrator Model 3393A was used to integrate and record the output of the detector. Details of liquid sample analysis are given in Appendix A.

Catalyst Analysis. The catalyst was analyzed by a Quantachrome Autoscan Porosimeter before and after the reaction to determine both its surface area and pore volume. The instrument consisted of an Autoscan Porosimeter Micro-Computer Data Acquisition and Reduction system and the filling apparatus. The Data Acquisition system had a complete Z80 micro-computer with a control program in its ROM while the data was stored in the RAM. The filling apparatus included a sample cell, a vacuum pump and a stainless steel sheath. In order to measure the pore volume and the surface area, the mercury penetration method was used. This method was based on the fact that mercury had a significant surface

tension and did not wet the catalyst surface.

The used catalyst was also analyzed to determine the deposited coke on the catalyst surface. At first, the catalyst was extracted with tetrahydrofuran in a Soxhlet apparatus for about 24 hours until the adhering soluble hydrocarbons were removed from the catalyst surface by the solvent. After drying under atmospheric conditions for 12 hours, the catalyst was burned at 550 °C (1022 °F) in a muffle furnace for 60 hours. After burning, the catalyst weight was measured. The catalyst weight was expected to decrease by the amount of the deposited coke. But in this project, the catalyst weight increased after burning. This meant that the chemical structure of the catalyst changed during the regeneration process. This structural change was later confirmed through Scanning Electron Microscopy (SEM) and Energy Dispersion Spectrometer (EDS). More details are presented in Chapters IV and V.

Experimental Techniques

For this experiment, a mixture of 10 wt.% quinoline in n-hexadecane was hydrotreated in the reactor over the unsupported molybdenum nitride powders under a hydrogen pressure of 10.4 MPa (1500 psig) and at a temperature range of 270 - 330 °C (518 - 626 °F). Samples of reaction products were taken at specific time intervals of 1 hour and analyzed by the GC.

During this work, two modes of operations were used, a

flow system and a non-flow system. In the flow system, hydrogen gas flowed continuously from cylinder to the reactor and a small amount of gases was vented to the atmosphere. This method was found to be inappropriate for kinetic study, because of the loss of the vaporized quinoline. The non-flow system was used to collect all the reported data in this work. In this case, the reactor was maintained under constant pressure of hydrogen without venting any of the gases out of the reactor.

The catalyst was placed in the glass liner in the reactor and the mixture of quinoline and n-hexadecane was added. The system was assembled and pressurized to 1500 psig with nitrogen gas to check any leaks. A Pressure drop of less than 50 psi per hour was considered as an acceptable leak. After adjusting the wall temperature of the reactor to 80 ^{o}C higher than the desired reaction temperature, heating was carried out for 3 hours. In order to start the reaction, the inert nitrogen gas was replaced by hydrogen gas. The reactor was depressurized to 1000 psig by opening the vent carefully and then pressurized to 1500 psig with hydrogen. The procedure was repeated for about ten times in about 30 minutes to ensure complete removal of nitrogen from the reactor system. Finally the reactor was pressurized with hydrogen to the reaction pressure (1500 psig) and a liquid sample was taken. This sample was labeled as sample number zero and considered to represent the starting point of the reaction. The required pressure and temperature were con-

trolled and maintained constant during the reaction. Periodically, liquid samples were taken at specified time intervals (1 hour) through the sampling valve and the sampling cylinder. To take a liquid sample, the stirrer was turned off to allow catalyst particles to settle. The sampling cylinder and the sampling line between the reactor and the sampling cylinder were pressurized to 1000 psig. Then the sampling valve 18 was opened slightly so that the pressure of the sampling system became about 1300 psig. Thus samples were taken from the reactor by the effect of pressure difference. At the end of reaction time, the system was shut down and the reactor was quenched under the reaction pressure with nitrogen. After cooling for a day, the reactor system was opened and the used catalyst was separated for analysis.

One of the operational problems was the solidification of the n-hexadecane in the lines during cold days, because the melting point of this solvent is 17 ^{o}C. This problem was solved by heating the sampling lines with electric heating tapes. Details of all experimental procedures are given in Appendix B.

CHAPTER IV

EXPERIMENTAL RESULTS

In this chapter, the results of analysis of the liquid and catalyst samples are presented. In this project, a total of 18 experimental runs were conducted, including a few duplicated runs, which are summarized in Table I. The results of only seven of these runs are reported here, because the rest of the runs were either in flow-mode or were not completed because of technical difficulties. Table II shows the experimental conditions of these runs. For the catalytic runs, about 3-5 g of the catalyst were added to a mixture of 10 wt.% quinoline in n-hexadecane to conduct the experiment. The reaction temperature was varied in the range of 270 - 330 °C (518 - 626 °F) while the pressure was maintained constant at 10.4 MPa (1500 psig). The starting amount of the mixture was 250 g and its volume was 313 cm^3. The duration of all experiments were 12 hours except where technical problems prohibited it. The liquid samples were taken in 1 hour intervals. The material balance was checked in these experiments and the average compound loss for these 7 experimental runs was 5.7 % of the initial amount of the mixture. One duplicated run (Run No. 5) in which liquid samples were taken every 2 hours was conducted to collect

TABLE I

SUMMARY OF ALL EXPERIMENTS*

Consecutive Run No.	Temp. (°C)	Duration (hr)	Catalyst wt. (g)	Comments
C1	330	2	-	. inadequate liquid feed . gas-flow system
C2	300	4	-	. increased the feed to 250 g . gas-flow system
C3	300	4	5	. heating difficulty . gas-flow system
C4	300	8	-	. 3 hours heating . increased run time . gas-flow system
C5	300	4	-	. feed discharged by mistake
C6	300	16	-	. quinoline lost to flowing gas
C7	300	12	-	. no gas flow . no reaction due to N_2 atmosphere
C8	330	12	-	. no reaction due to N_2 atmosphere
C9	300	12	-	. no gas flow . N_2 changed to H_2 . run number 2
C10	330	11	-	. run number 3
C11	360	12	-	. temp. too high
C12	270	11	-	. run number 1

TABLE I (Continued)

Consecutive Run No.	Temp. (°C)	Duration (hr)	Catalyst wt. (g)	Comments
C13	270	12	-	. duplicate of run number C12
C14	270	-	5	. temp. controller malfunction
C15	270	11	5	. run number 4
C16	300	11	5	. duplicate of run number C19
C17	330	12	5	. run number 6
C18	300	12	3	. run number 7
C19	300	12	5	. run number 5

* All experiments were conducted under the constant reaction pressure of 10.4 MPa (1500 psig)
* The stirrer speed was maintained constant at 650 r.p.m.

TABLE II

EXPERIMENTAL REACTION CONDITIONS*

Run No.	Temperature (°C)	Catalyst wt. (g)	Duration (hr.)	compound loss (wt.%)
1	270	0	12	6.00
2	300	0	12	6.56
3	330	0	11	9.17
4	270	5	11	4.00
5	300	5	12	6.00
6	330	5	12	5.88
7	300	3	12	2.60

* Reaction Pressure : 10.4 MPa (1500 psig)

data for the reaction at 300 °C with 5 g of the catalyst.

Liquid Sample Analysis

In order to evaluate the catalytic properties of molybdenum nitride in quinoline hydrogenation, the product samples from catalytic reactions were analyzed and compared with those from noncatalytic reactions. The unique hydrocarbon product of both catalytic and noncatalytic reactions was identified as Py-THQ, known as the most basic species among the intermediates of quinoline HDN. No attempt was made to identify and measure the possible cracking products of n-hexadecane because the major peaks in gas chromatogram were those of quinoline, Py-THQ, n-hexadecane, and impurites in n-hexadecane. The other peaks were insignificant (Figure 4).

The liquid samples of both catalytic and noncatalytic reactions were analyzed to measured the concentrations of quinoline, Py-THQ, and n-hexadecane. These concentrations as a function of time at each reaction temperature are tabulated in Tables III - V and shown in Figures 5 - 7. In these Tables and Figures, run hour zero indicates the starting point of the reactions when the initial sample was taken after displacing nitrogen with hydrogen gas.

The concentration of quinoline in the original mixtures was 10 wt %, which decreased to less than its original value by the time the initial sample was taken. This decrease was the result of vaporization of some of the quinoline into the

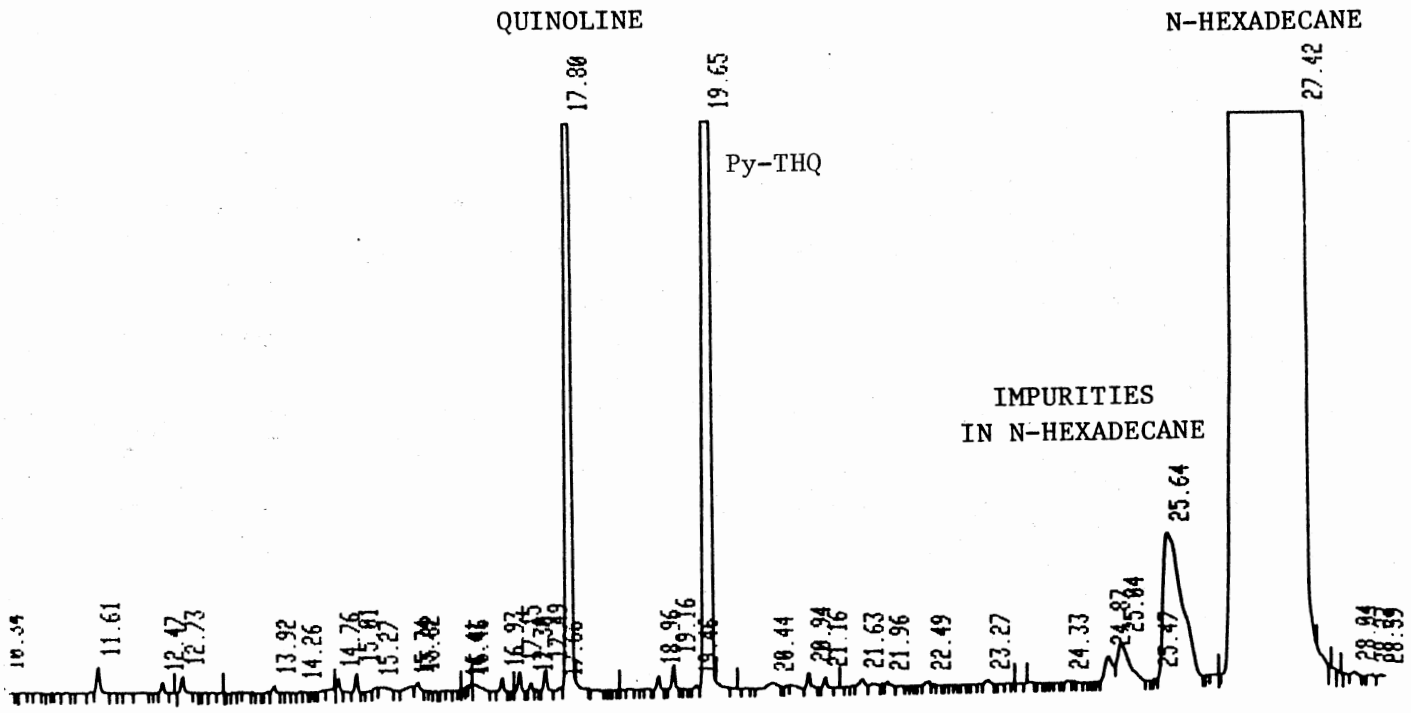

Figure 4. A Typical Chromatogram for Quinoline HDN Products over Molybdenum Nitride at 330 C (Run No. 6, 6hr)

TABLE III

RESULTS OF ANALYSIS OF LIQUID SAMPLES
OF RUN NO. 1 and 4 (270 °C) IN WT. %

Run Time (hr.)	Noncatalytic (Run No.1)		Catalytic (Run No.4)	
	Quinoline	Py-THQ	Quinoline	Py-THQ
0	5.92	0.01	6.51	0.05
1	4.77	0.01	3.92	0.14
2	4.07	0.01	3.58	0.24
3	4.28	0.02	3.89	0.34
4	4.16	0.02	4.23	0.39
5	4.36	0.02	4.44	0.45
6	4.34	0.03	4.48	0.50
7	4.25	0.04	4.53	0.54
8	4.55	0.05	4.50	0.56
9	4.36	0.05	4.91	0.60
10	4.40	0.06	5.74	0.77
11	4.69	0.07	5.24	0.76
12	5.67	0.08	*	*

* Liquid sample was not available

TABLE IV

RESULTS OF ANALYSIS OF LIQUID SAMPLES
OF RUN NO. 2, 5, AND 7 (300 °C) IN WT. %

Run Time (hr.)	Noncatalytic (Run No.2)		Catalytic* (Run No.7)		Catalytic** (Run No.5)	
	Q***	Py-THQ	Q***	Py-THQ	Q***	Py-THQ
0	6.62	0.04	8.59	0.05	9.28	0.14
1	4.87	0.09	7.50	0.28		
2	4.66	0.16	5.91	0.34	4.95	0.46
3	3.80	0.27	4.31	0.42		
4	3.55	0.33	3.55	0.48	3.56	1.01
5	3.34	0.40	3.81	0.68		
6	3.31	0.49	3.66	0.94	3.43	1.79
7	3.45	0.60	3.73	1.27		
8	3.83	0.76	3.57	1.50	2.93	2.01
9	3.60	0.85	3.60	1.88		
10	3.77	0.94	3.28	2.22	2.06	2.21
11	4.56	1.17	3.18	2.41		
12	4.96	1.27	3.21	2.48	1.97	2.74

* The amount of catalyst was 3 g
** The amount of catalyst was 5 g and liquid samples were taken in every 2 hours
*** Quinoline

TABLE V

RESULTS OF ANALYSIS OF LIQUID SAMPLEW
OF RUN NO. 3 AND 6 (330 °C) IN WT. %

Run Time (hr.)	Noncatalytic (Run No.3)		Catalytic (Run No.6)	
	Quinoline	Py-THQ	Quinoline	Py-THQ
0	7.40	0.15	8.55	0.23
1	5.17	0.15	7.05	0.75
2	4.16	0.33	5.09	1.77
3	3.77	0.50	2.97	2.50
4	3.53	0.64	2.32	2.74
5	3.42	0.83	1.81	3.12
6	3.25	1.10	1.41	3.78
7	3.14	1.26	1.07	4.40
8	3.00	1.45	0.81	5.02
9	3.53	1.97	0.57	5.29
10	4.38	2.38	0.45	5.97
11	4.58	3.10	0.34	5.93
12	*	*	0.30	6.35

* Liquid sample was not available

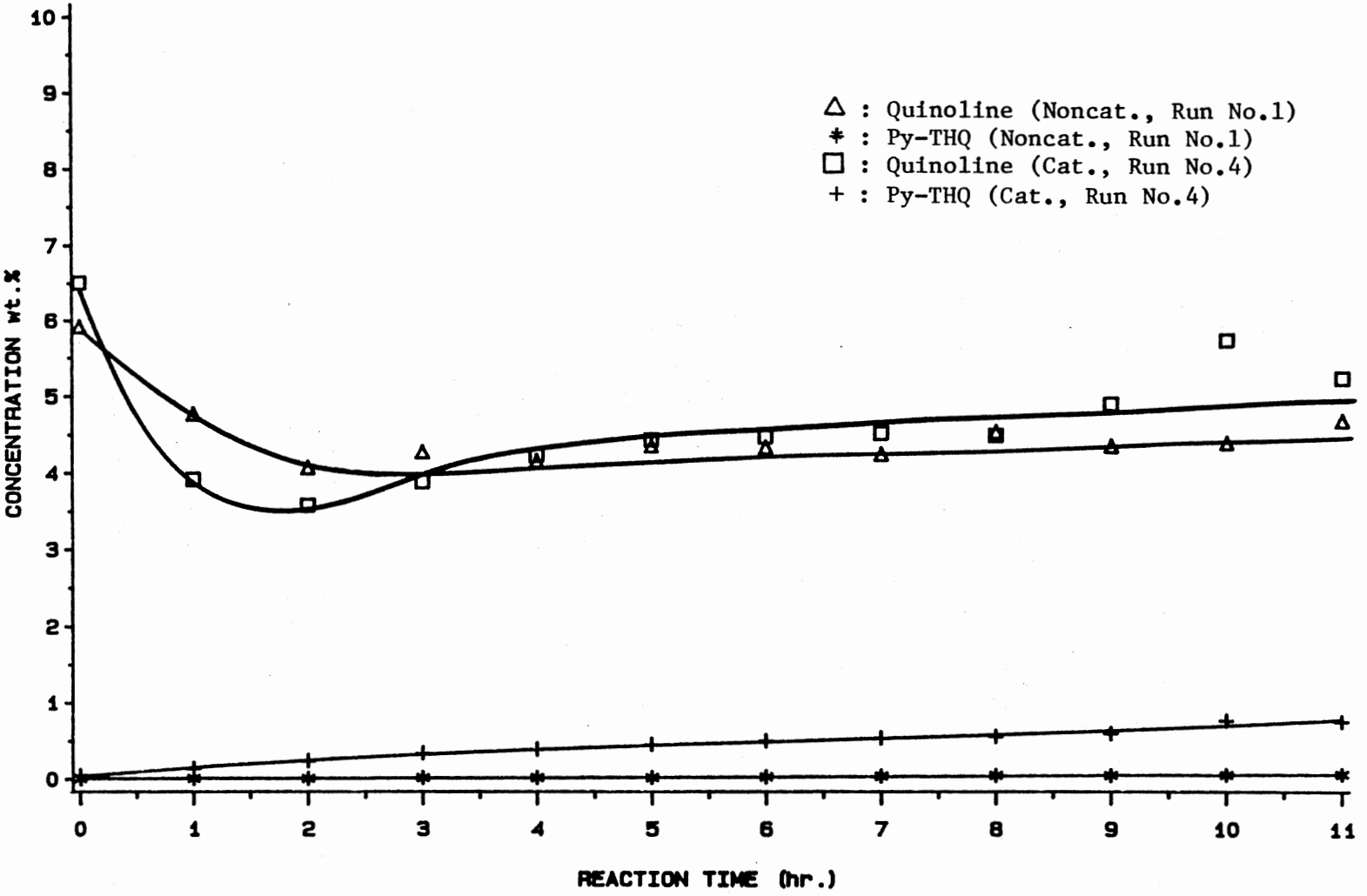

Figure 5. Conversion of Quinoline to Py-THQ in Runs No. 1 and 4 (270 C)

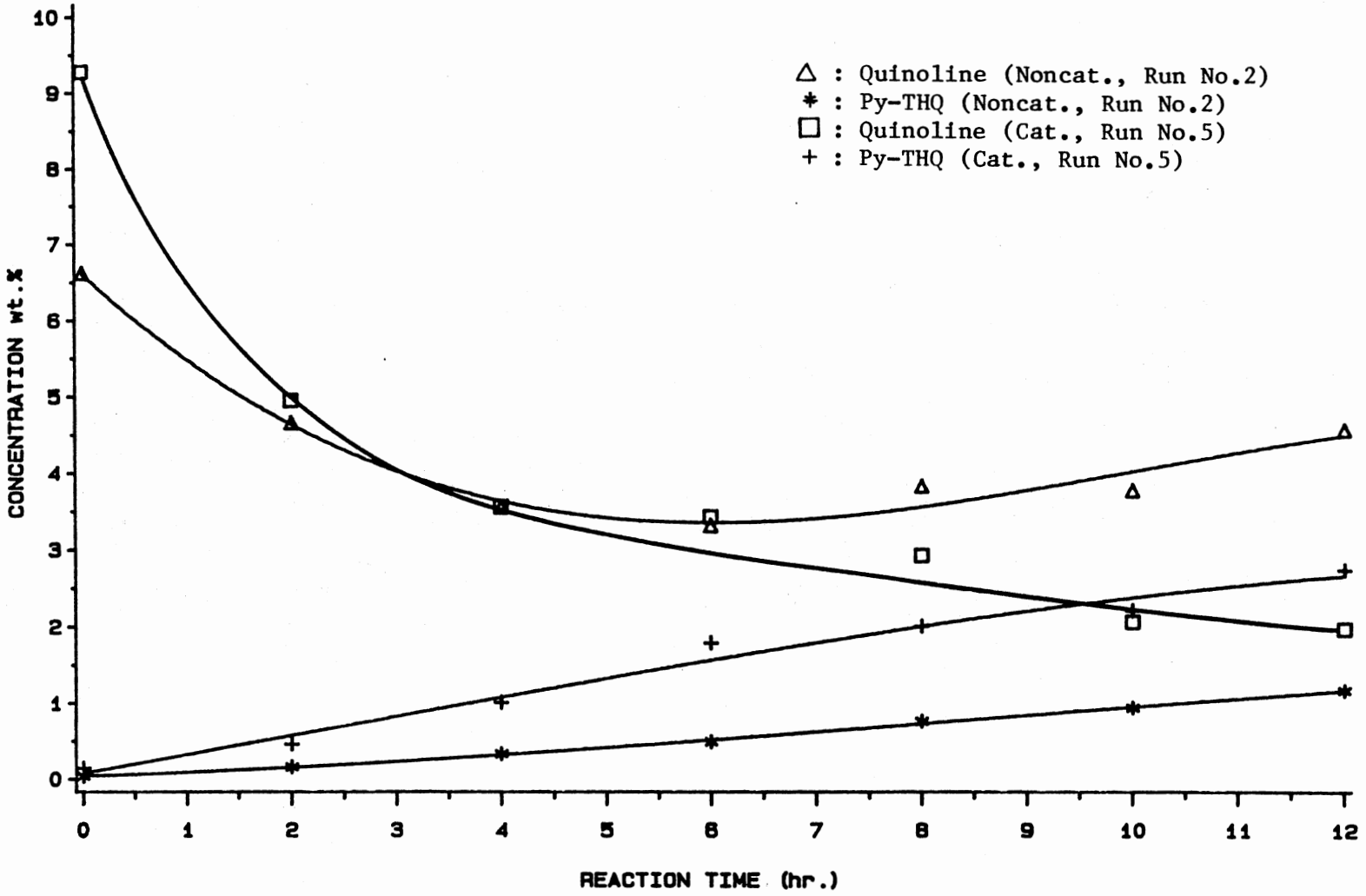

Figure 6. Conversion of Quinoline to Py-THQ in Runs No. 2 and 5 (300 C)

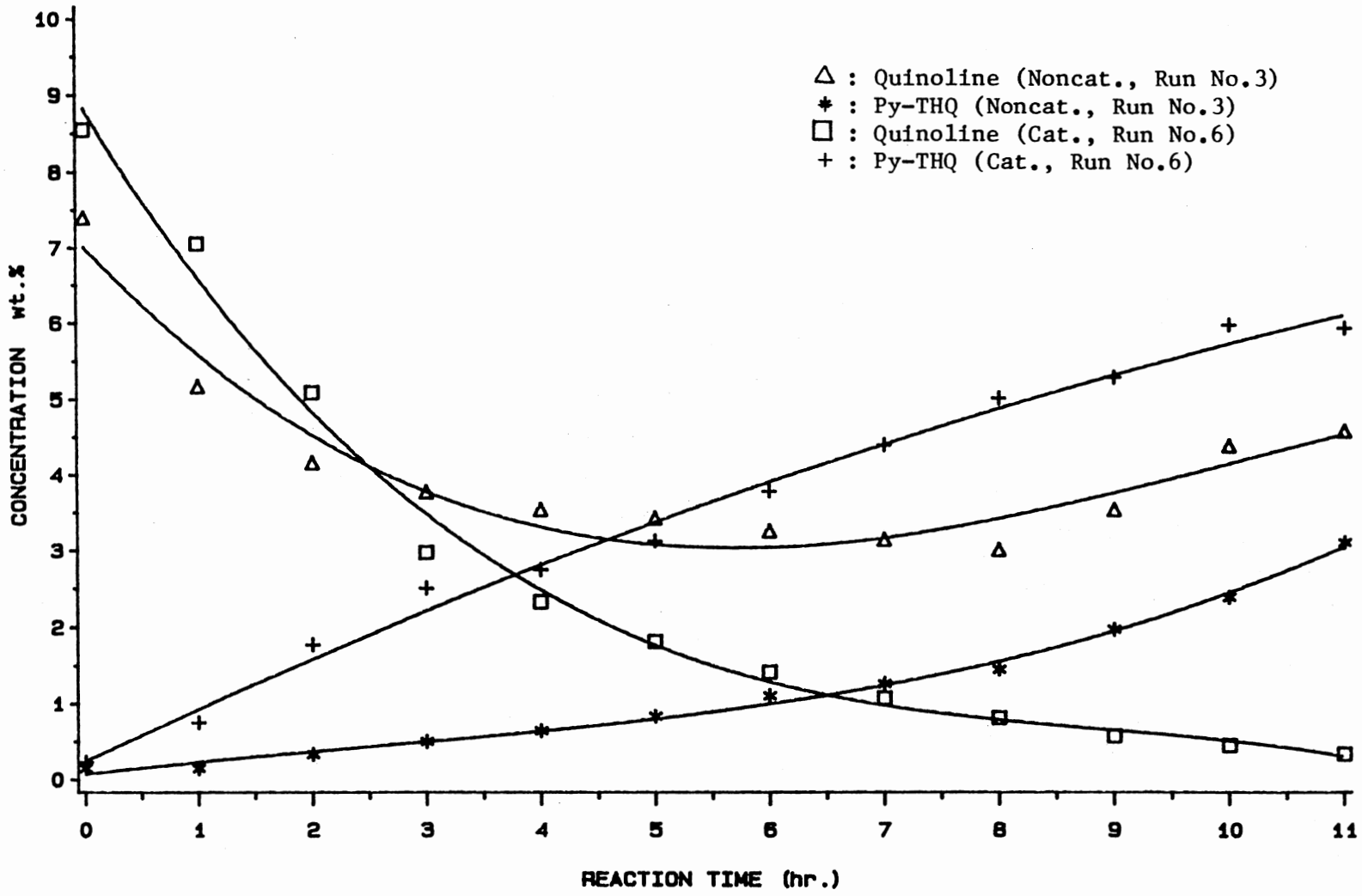

Figure 7. Conversion of Quinoline to Py-THQ in Runs No. 3 and 6 (330 C)

gas phase during heating period. In replacing nitrogen by hydrogen after heating the reactor, the vaporized quinoline was lost with the vented nitrogen and hydrogen causing further evaporation of quinoline. This was confirmed by the rapid decrease of the amount of quinoline in the first 1-2 hours of the reaction. Some of the quinoline reacted with hydrogen during replacing nitrogen with hydrogen, thus Py-THQ concentration is not zero at the starting point or zero time.

During the last 2-3 hours of the reaction, it was observed that the concentration of both quinoline and Py-THQ increased. This could be explained by considering that the quinoline which initially evaporated into the vapor phase redesolved in the liquid and entered into the liquid samples. The total amount of quinoline and Py-THQ at the start and the end of the run remained nearly constant, while for mid-run samples, this total amount in the liquid was lower than its value at the start of the run.

At 270 °C, about 11.6 % of quinoline was converted to Py-THQ in catalytic run (Run No. 4) whereas only 1.27 % was converted in noncatalytic run (Run No. 1). As shown in Figure 5 and Table III, there were no other products in both catalytic and noncatalytic reactions. Within the duration of the reaction, the wt.% of Py-THQ increased almost steadily, which meant that the reaction did not reach equilibrium state.

At 300 °C, the products of both catalytic

(Run No. 5 and 7) and noncatalytic (Run No. 2) runs were the same as those at 270 °C but the rates of conversion of quinoline and of formation of Py-THQ were higher than those at 270 °C. At this temperature, the effect of the amount of the catalyst on the reaction was also measured. The concentration of Py-THQ increased with increasing the amount of the catalyst, as seen in Table IV and Figure 8. The maximum conversion of quinoline to Py-THQ within the duration of the reaction was 41.9 % in the experiment with 3 g catalyst (Run No. 7) and 54.5 % with 5 g catalyst (Run No. 5) compared with 19.3 % in the noncatalytic reaction (Run No. 2). Figure 6 shows the concentrations of quinoline and Py-THQ in the experiment with 5 g catalyst at 300 °C. The reaction at this temperature did not reach chemical equilibrium, either.

At 330 °C, 91.7 % of quinoline was converted into Py-THQ in the catalytic run (Run No. 6). Py-THQ was again identified as the sole product of both catalytic and noncatalytic runs (Run No. 3). While the conversion was only 37.8 % in the noncatalytic experiment. As can be seen in Table V and Figure 7, the concentration of Py-THQ increases steadily which means that the equilibrium state is not attained at this temperature within the reaction times.

In order to clearly show the effect of temperature, the weight percent versus time plots for Py-THQ are shown in Figures 9 and 10. Figure 9 presents the wt.% of Py-THQ profile in the noncatalytic run and Figure 10 shows a similar

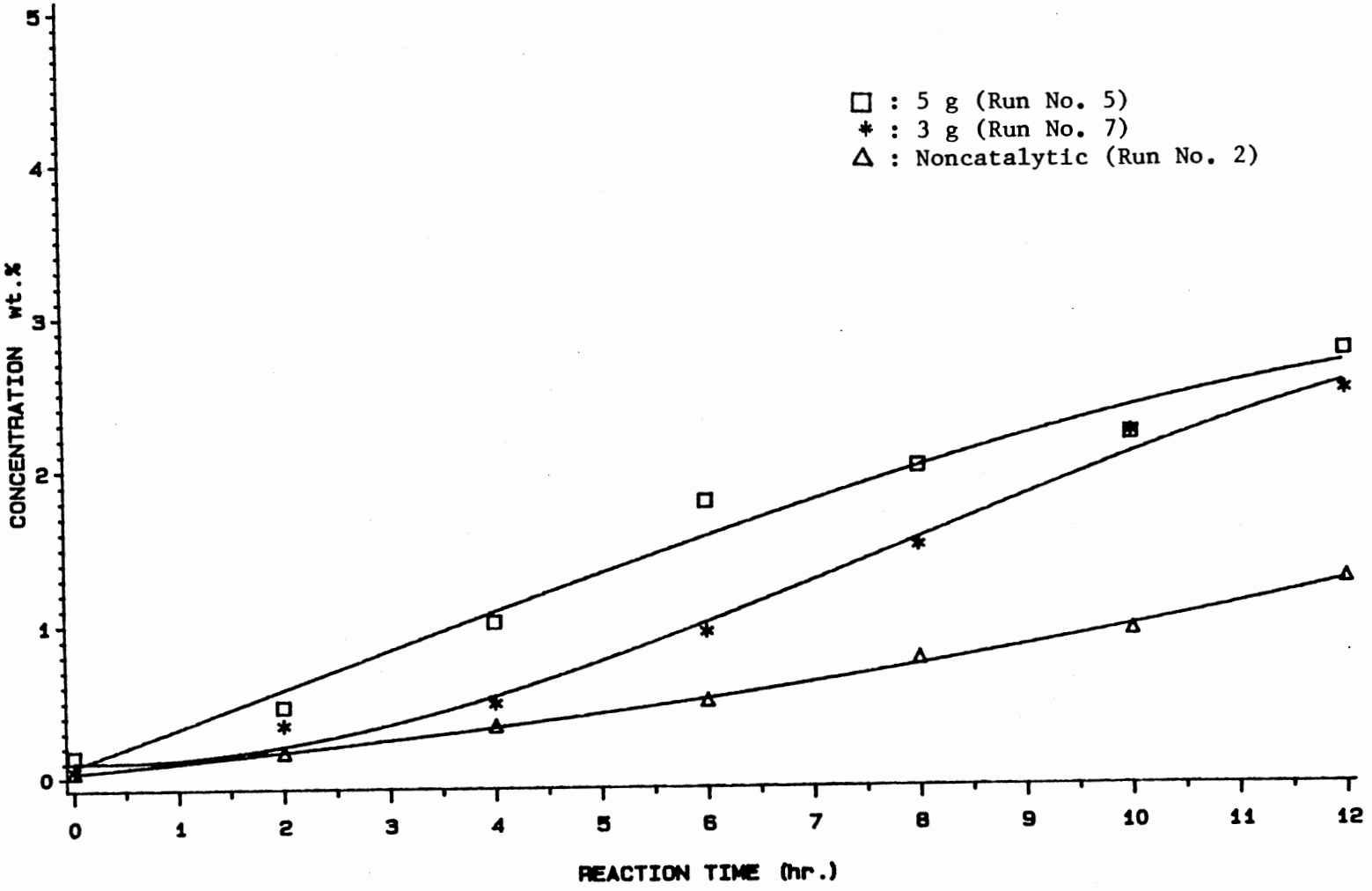

Figure 8. Effect of the Amount of the Catalyst on the Formation of Py-THQ at 300 C (Run No. 2, 5, and 7)

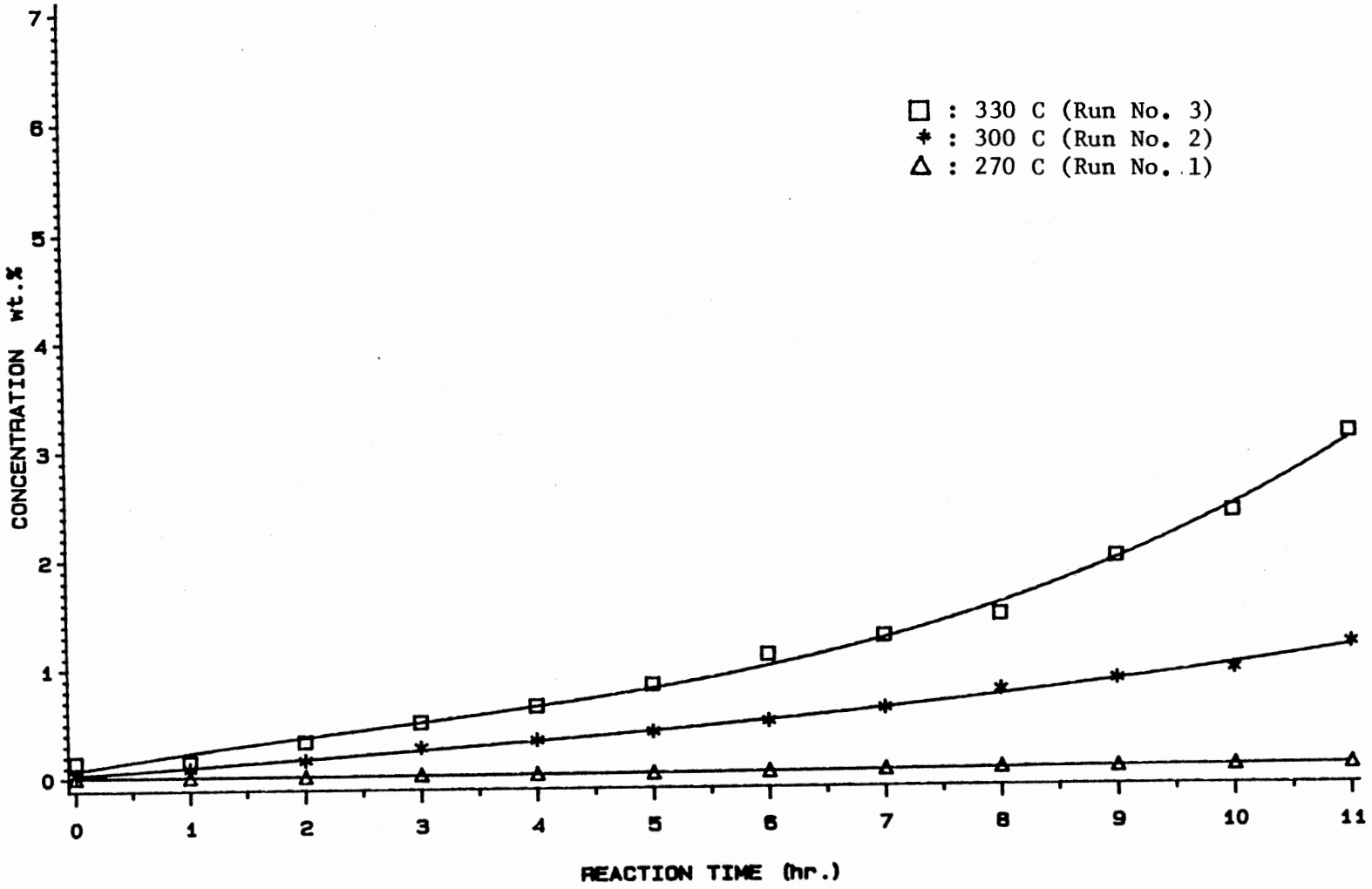

Figure 9. Effect of Temperature on the Formation of Py-THQ in Noncatalytic Reactions (Run No. 1, 2, and 3)

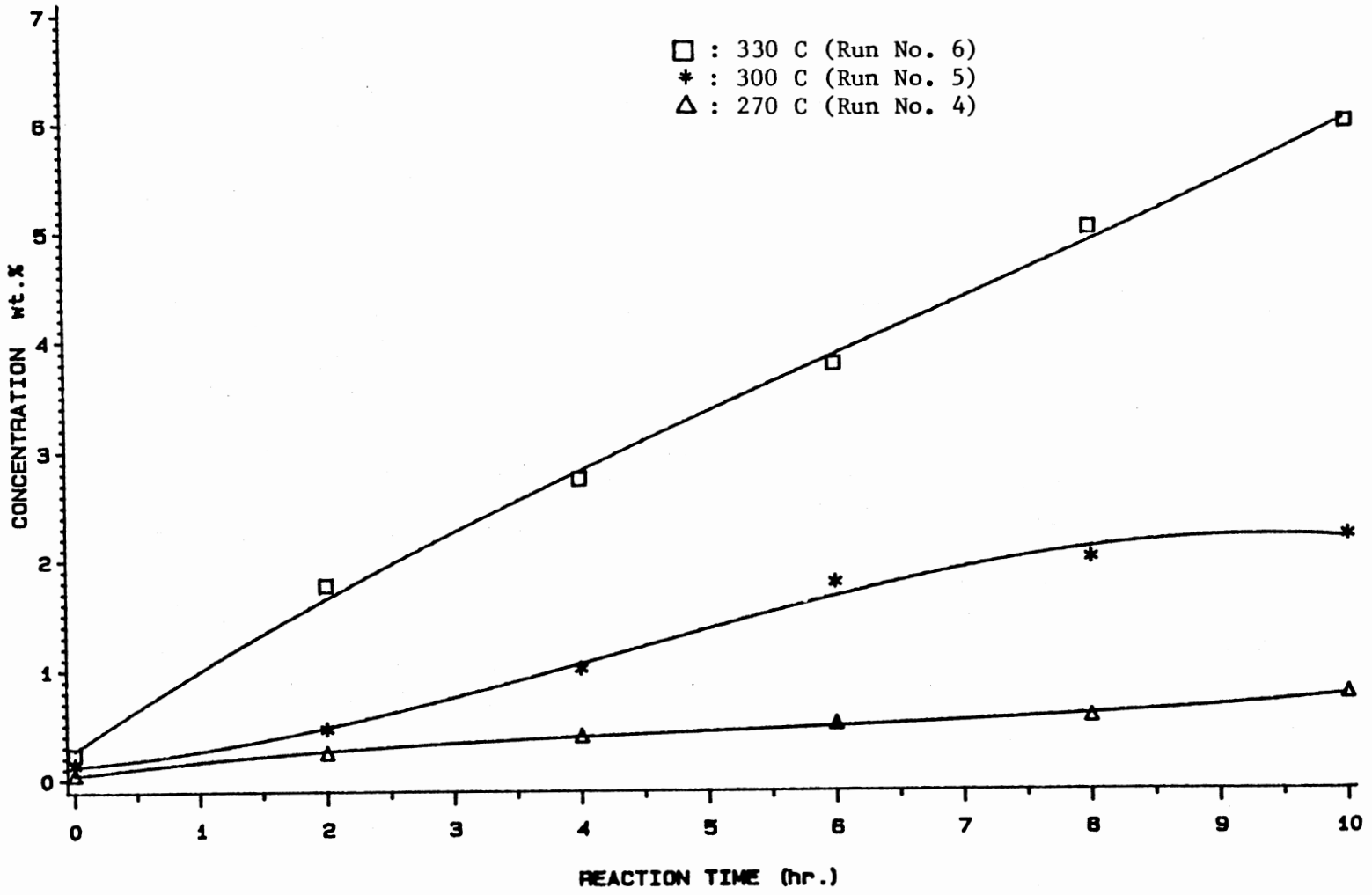

Figure 10. Effect of Temperature on the Formation of Py-THQ in Catalytic Reactions (Run No. 4, 5, and 6)

plot for the catalytic reaction. It is apparent that increasing temperature increases the rate of quinoline conversion and at these temperatures, the unique product of both catalytic and noncatalytic reactions is Py-THQ.

All experimental data in weight percent were rearranged in molar units and are shown in Tables VI - VIII. These data were used to calculate the conversion, Xa, as a function of time and to study the kinetic model discussed in Chapter V. Details of the calculation procedures are presented in Appendix C.

Catalyst Analysis

The chemical composition and physical properties of molybdenum nitride powders used in this project are shown in Table IX. The catalyst used at 300 °C (Run No.5) was analyzed for surface area and pore volume and was burned to measure its coke content. After burning at 550 °C (823 °K) for 60 hours, the catalyst was weighed, then analyzed for surface area and pore volume to compare with those of the fresh catalyst. The fresh catalyst was burned at the same conditions and analyzed similarly in order to find the effects of burning on the properties of the catalyst. The results are presented in Tables X and XI.

Table X shows an interesting and unexpected phenomena. The catalyst weight increased and its color changed from black to yellow green after burning. This indicates changes in chemical composition of the catalyst during combustion.

TABLE VI

RESULTS OF ANALYSIS OF LIQUID SAMPLES
OF RUNS NO. 1 AND 4 (270 °C)

RUN NO. (Amount of Cat.,g)	Time (hr)	Moles of Quinoline	Moles of Py-THQ	Fractional Conversion
1 (0)	0	0.100	0	0
	1	0.078	<0.001	0.001
	2	0.064	<0.001	0.001
	3	0.065	<0.001	0.003
	4	0.061	<0.001	0.004
	5	0.062	<0.001	0.003
	6	0.059	<0.001	0.006
	7	0.056	<0.001	0.008
	8	0.057	0.001	0.010
	9	0.052	0.001	0.010
	10	0.051	0.001	0.012
	11	0.052	0.001	0.013
	12	0.063	0.001	0.013
4 (5)	0	0.111	0	0
	1	0.065	0.001	0.022
	2	0.058	0.003	0.049
	3	0.060	0.004	0.067
	4	0.063	0.005	0.072
	5	0.064	0.006	0.080
	6	0.063	0.006	0.088
	7	0.062	0.006	0.095
	8	0.058	0.006	0.099
	9	0.060	0.006	0.098
	10	0.069	0.008	0.108
	11	0.062	0.008	0.116

TABLE VII

RESULTS OF ANALYSIS OF LIQUID SAMPLES
OF RUNS NO. 2, 5, AND 7 (300 °C)

RUN NO. (Amount of Cat.,g)	Time (hr)	Moles of Quinoline	Moles of Py-THQ	Fractional Conversion
2 (0)	0	0.112	0	0
	1	0.080	0.001	0.010
	2	0.074	0.002	0.025
	3	0.058	0.003	0.055
	4	0.052	0.004	0.074
	5	0.047	0.005	0.095
	6	0.045	0.006	0.116
	7	0.045	0.007	0.135
	8	0.047	0.009	0.154
	9	0.042	0.009	0.178
	10	0.043	0.010	0.187
	11	0.050	0.012	0.193
	12	0.054	0.013	0.193
7 (3)	0	0.145	0	0
	1	0.124	0.004	0.028
	2	0.095	0.004	0.045
	3	0.068	0.006	0.075
	4	0.054	0.006	0.103
	5	0.056	0.009	0.136
	6	0.052	0.012	0.188
	7	0.051	0.016	0.238
	8	0.047	0.018	0.279
	9	0.046	0.022	0.327
	10	0.040	0.025	0.387
	11	0.037	0.026	0.414
	12	0.035	0.025	0.419
5 (5)	0	0.117	0	0
	2	0.061	0.004	0.059
	4	0.043	0.010	0.185
	6	0.040	0.018	0.310
	8	0.033	0.020	0.370
	10	0.023	0.021	0.477
	12	0.021	0.025	0.545

TABLE VIII

RESULTS OF ANALYSIS OF LIQUID SAMPLES
OF RUNS NO. 3 AND 6 (330 °C)

RUN NO. (Amount of Cat.,g)	Time (hr)	Moles of Quinoline	Moles of Py-THQ	Fractional Conversion
3 (0)	0	0.125	0	0
	1	0.090	0.000	0.002
	2	0.073	0.003	0.040
	3	0.067	0.006	0.081
	4	0.062	0.008	0.116
	5	0.061	0.012	0.167
	6	0.058	0.016	0.214
	7	0.056	0.018	0.248
	8	0.053	0.021	0.287
	9	0.062	0.030	0.325
	10	0.076	0.036	0.324
	11	0.078	0.048	0.378
6 (5)	0	0.144	0	0
	1	0.121	0.008	0.065
	2	0.089	0.025	0.219
	3	0.054	0.037	0.408
	4	0.043	0.041	0.488
	5	0.035	0.047	0.579
	6	0.028	0.058	0.677
	7	0.022	0.068	0.757
	8	0.018	0.078	0.817
	9	0.013	0.083	0.860
	10	0.011	0.093	0.891
	11	0.010	0.093	0.907
	12	0.009	0.099	0.917

TABLE XI

PROPERTIES OF MOLYBDENUM NITRIDE POWDER

Chemical Composition	Mo_2N + MoN*
Appearance	black powder
Surface Area, m^2/g cat.	1.80 **
Pore Volume, cm^3/g cat.	0.25 **
Average Particle Size, mm	0.05 ***
Specific Gravity	9.06*
Vendor	Alfa Products

* From vendor's data
** Measured by mercury penetration method in our laboratory.
*** Measured by Scanning Electron Microscopy (SEM)

TABLE X

WEIGHT INCREASE AFTER BURNING OF CATALYST

Catalyst	Before burning (g)	After burning (g)	Weight increase (g/g cat.)
Fresh	0.83	1.16	0.39
	0.67	0.91	0.36
Used*	0.56	0.76	0.36
	0.13	0.18	0.38

* Used at 300 °C (Run No. 5)

TABLE XI

CHANGES IN PHYSICAL PROPERTIES OF CATALYST AFTER BURNING

	Fresh Catalyst		Used Catalyst*	
	Before burning	After burning	Before burning	After burning
Pore Volume (cm^3/g cat.)	0.25	0.30	0.18	0.35
Surface Area (m^2/g cat.)	1.80	16.0	5.90	6.40

* Used at 300 °C (Run No. 5)

It is postulated that molybdenum nitride is oxidized to molybdenum oxide during burning at high temperature. Another interesting observation from Table XI is that the physical properties of the fresh catalyst and the used catalyst after burning were quite different from those measured before combustion. The surface area of the catalyst after the reaction increased to about three times as much as that of the fresh catalyst. Meanwhile there was a small increase in the pore volume and a dramatic increase in the surface area of the fresh catalyst after combustion. Whereas, the surface area of the used catalyst increased only slightly when compared with that of the fresh catalyst. This indicates that something happens to the surface of the catalyst during the reaction. The changes in physical properties of the catalyst during the reaction and regeneration process were confirmed by Scanning Electron Microscopy (SEM) and are discussed in detail in Chapter V. Also discussed in that chapter are the changes in chemical composition of the catalyst shown during the combustion process.

CHAPTER V

DISCUSSION OF RESULTS

In this chapter, the results of analysis of the liquid samples are discussed and a kinetic model is developed to fit the experimental data. The results of the catalyst analysis are also discussed. The catalytic properties of molybdenum nitride are evaluated by comparing the rate constants and activation energies obtained from the catalytic reactions with those obtained from the reaction over sulfided CoMo/alumina and NiMo/alumina catalysts.

Selective Hydrogenation of Quinoline

From the results of analysis of the liquid samples, the unique product of the catalytic and noncatalytic hydrogenation of quinoline was Py-THQ, which is known to be the most basic species among the intermediates of quinoline HDN. This indicates that molybdenum nitride selectively hydrogenates only the pyridine side of the quinoline and that it does not have the ability to remove the nitrogen atom from quinoline at the reaction conditions of the present work.

Many of the early investigators of the hydrogenation of quinoline reported that Py-THQ can be obtained selectively from hydrogenation of quinoline over nickel, nickel-

aluminum, platinum oxide in ethanol, copper, tungsten trioxide-nickel oxide-alumina, and tungsten disulfide-alumina catalysts at relatively low temperatures of 80 - 250 °C. Molybdenum based catalysts have been known to be excellent hydrotreatment catalysts for coal liquids, especially if promoted by cobalt or nickel. In fact, it is believed that the two different reactions in the quinoline HDN, i.e. hydrogenation and hydrogenolysis, occur at different catalyst sites. Yang and Satterfield (1983) proposed that Brönsted acid sites on the catalyst surface are responsible for hydrogenolysis, cracking, and isomerization and that the presence of sulfur atoms favors hydrocracking while inhibiting hydrogenation. Schrader and Cheng (1983) suggested that the molybdenum oxide species form aggregated or polymeric species on the surface of the aluminum oxide support which are responsible for the Brönsted acidity. Suarez, et al. (1983) detected the presence of both Lewis and Brönsted acid sites on the Mo/alumina catalyst surface, whereas only Lewis sites were found on the alumina surface, which are believed to be responsible for the hydrogenation. From the previous studies, molybdenum nitride is expected to possess both the hydrogenation and hydrogenolysis sites. The selectivity shown by this catalyst in the present experiment may result from the interaction between nitrogen atom of quinoline and the surface of the catalyst. It has been reported that quinoline is rapidly hydrogenated to an equilibrium amount of Py-THQ over presulfided commercial HDN

catalysts. According to the work of El-Bishtawi (1986), quinoline concentration decreases to less than 10 % in the first hour of the reaction over 5.4 g of NiMo/alumina catalyst at 357 °C and is mainly converted to Py-THQ with the formation of a small amount of Bz-THQ. After this time, the rate of quinoline conversion and the rate of the formation of Py-THQ both decrease, due to the chemical equilibrium. In the present work, catalytic conversion of quinoline was found to be favored by both high temperatures and increased amount of the catalyst, as shown in Figures 8-10. At three different reaction temperatures, the conversions were 11.6 %, 47.7 %, and 91.8 % after the first 11 hours at 270, 300, and 330 °C, respectively (Tables VI, VII, and VIII). The conversions kept increasing with the reaction time.

Cocchetto (1976) studied the hydrogenation of quinoline and calculated the thermodynamic equilibrium constants of each step in the quinoline HDN reaction network by estimating the free energy of formation for the unsaturated and saturated heterocyclic nitrogen compounds. Based on a modified Van Krevelen method, which could be in error by several kcal/mol, the fractional equilibrium conversion of quinoline to Py-THQ was obtained as 0.94, 0.85, and 0.65 at 270, 300, and 330 °C, respectively. However, a discrepancy is found in his data when they are compared with those from the present work. At 330 °C, quinoline conversion from this work is beyond the calculated equilibrium conversion and the conversion continues to increase. This inconsistency was also

observed by El-Bishtawi (1986) who claimed that the equilibrium conversion was not affected significantly by temperature. Later, Satterfield, et al. (1978) obtained the thermodynamic equilibrium constants of each step by experimental studies and suggested that the Cocchetto's data should be high by a value of log K of about 1.5 in the whole range of temperature. According to Satterfield's data, the equilibrium conversions at the reaction temperatures are 0.998, 0.994, and 0.981 and these values are more reliable. In all reaction cases of this project, the equilibrium state was not attained within the reaction time. The rates of approach to equilibrium state over presulfided HDN catalysts are higher than the rate over the molybdenum nitride catalyst.

Volpe and Boudart (1986) studied the catalytic properties of molybdenum nitride in ammonia synthesis and observed the strong inhibition of the rate of ammonia synthesis by the product, ammonia, which is attributed to a large value of the binding energy (380 kJ/mol) of nitrogen atom to the catalyst surface. Satterfield, et al. (1981) reported in the quinoline HDN study that after initial equilibrium with Py-THQ, quinoline was prevented from adsorbing and reacting on the catalyst surface until the concentration of Py-THQ had decreased significantly. The active catalyst sites on the HDN catalysts, for hydrogenolysis as well as hydrogenation, are most likely to be acidic in nature. Adsorption of nitrogen compounds is believed to occur through interaction

of the basic nitrogen group with acidic sites on the catalyst, so the more basic nitrogen compounds are apt to be more strongly adsorbed. Since quinoline is a less basic compound than Py-THQ, the specific selectivity and the low activity of molybdenum nitride in the quinoline hydrogenation can be interpreted in terms of the high affinity of nitrogen atoms to the molybdenum nitride and competitive adsorption between quinoline and Py-THQ. The pyridine side of quinoline, where the nitrogen atom is located, is likely to have the priority for adsorption on the surface of molybdenum nitride rather than benzene side because of the high affinity of nitrogen atoms to the catalyst surface.

Cocchetto (1981) reported the significance of noncatalytic conversion of quinoline to Py-THQ. The formation of Py-THQ in noncatalytic reaction can be so significant that it must be considered in modeling the catalytic HDN reactions of quinoline. As seen in Tables III, IV, and V in Chapter IV, the amount of Py-THQ produced by noncatalytic conversion of quinoline increases with temperature and contact times. At high temperatures and long contact times, the amount of noncatalytically converted quinoline increases to more than one half of that of the catalytic reaction. This may lead to an inaccuracy in setting the kinetic model in terms of specific expressions such as Langmuir-Hinshelwood equation, if the data from the noncatalytic reaction are not considered in the model.

Kinetic Model

Pseudo-First Order Reversible Reaction Model

The overall hydrogenation reaction of quinoline is symbolically represented as ;

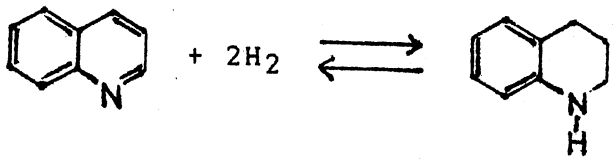

which may be expressed by the following equation ;

$$A + 2H_2 \underset{k2}{\overset{k1}{\rightleftharpoons}} B \qquad (1)$$

where A represents the reacting compound, quinoline and B is Py-THQ. If it is assumed that the reaction can be shown by a first order kinetic model, the rate of hydrogenation can be presented by;

$$r_A = - \frac{dC_A}{dt} = k_1 C_A P_{H2}^2 - k_2 C_B \qquad (2)$$

where r_A is the reaction rate, C_A and C_B are the concentrations of quinoline and Py-THQ at any time t, k_1 and k_2 are the forward and backward reaction rate constants, respectively, and P_{H2} is the partial pressure of hydrogen. Since the partial pressure of hydrogen is maintained as a constant during the reaction, equation (2) may be written as ;

$$r_A = - \frac{dC_A}{dt} = k' C_A - k_2 C_B \qquad (3)$$

where k' is the pseudo-first order rate constant. Equation (3) can also be presented in terms of the conversion, which is defined as the ratio of the amount of the reactant A converted to the initial amount of A.

$$\frac{dX_A}{dt} = k' (1-X_A) - k_2 X_A \qquad (4)$$

where X_A is the conversion of A into B at time t. At equilibrium, $dX_A / dt = 0$ and then;

$$\frac{k'}{k_2} = \frac{X_{Ae}}{(1-X_{Ae})} \qquad (5)$$

where X_{Ae} is the equilibrium conversion. If the equilibrium conversion is introduced into the equation (4), then, equation (4) will be modified as ;

$$\frac{dX_A}{dt} = k' \frac{(X_{Ae} - X_A)}{X_{Ae}} \qquad (6)$$

Integration of equation (6) subject to the initial condition of $X_A = 0$ at $t = 0$ gives;

$$X_{Ae} \ln(1 - X_A / X_{Ae}) = - k' t \qquad (7)$$

Based on this model, a plot of $X_{Ae} \ln(1 - X_A / X_{Ae})$ versus time should result in a straight line with a slope of -k'. Figures 11, 12, and 13 were plotted by using the experimental data and the equilibrium conversions from the works by Cocchetto, et al. (1976) and Satterfield, et al.(1978) at 270, 300, and 330 °C, respectively. These Figures show the relation between $-\ln(1 - X_A / X_{Ae})$ and time, t, which appears to be, especially after 3 hours, almost linear. The best estimates for k' of both catalytic and noncatalytic reactions are obtained by the least square fit of these data.

The raw experimental data of this project are shown in Tables VI, VII, and VIII. These data are used to calculate the values of k' and the percentage relative deviations of the predicted conversions from the actual conversions of quinoline at any time t. The results are given in Tables XII - XVI. The percentage relative deviations in Tables XIV-XVI indicate that except for the first 2 hours, this model fits the quinoline hydrogenation data satisfactorily. Figures 14, 15, and 16 show a comparison between the actual conversions with the predictions of the model. It is considered that the reaction system was not stabilized during the first 2-3 hours of runs. Tables XII and XIII, as expected, show that the rate constants in both catalytic and noncatalytic reactions increase with increasing reaction temperature.

The rate constants in the present catalytic reactions are greater than those in the noncatalytic reactions, which

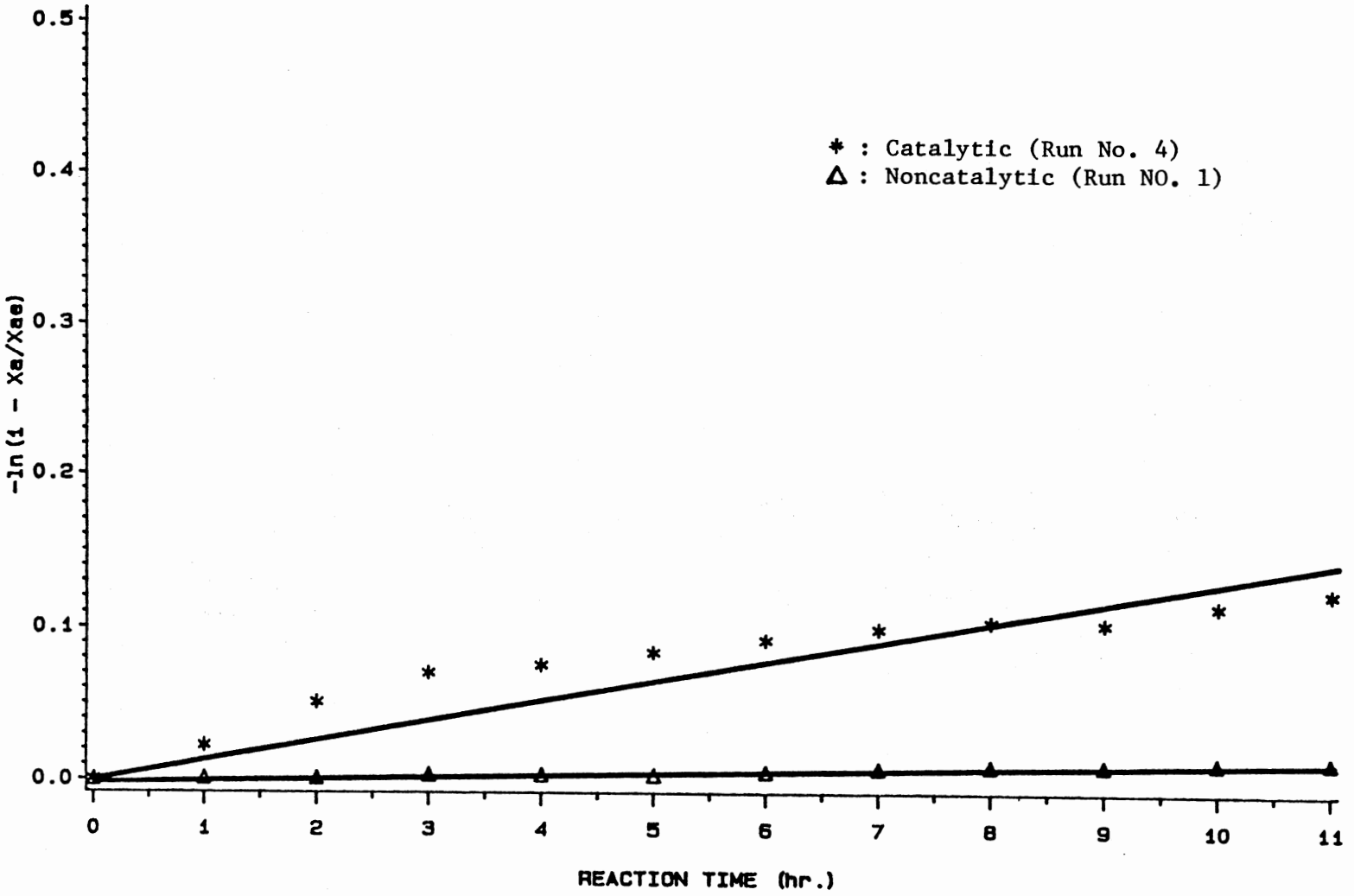

Figure 11. -ln (1-Xa/Xae) versus Time at 270 C
(Run No. 1 and 4)

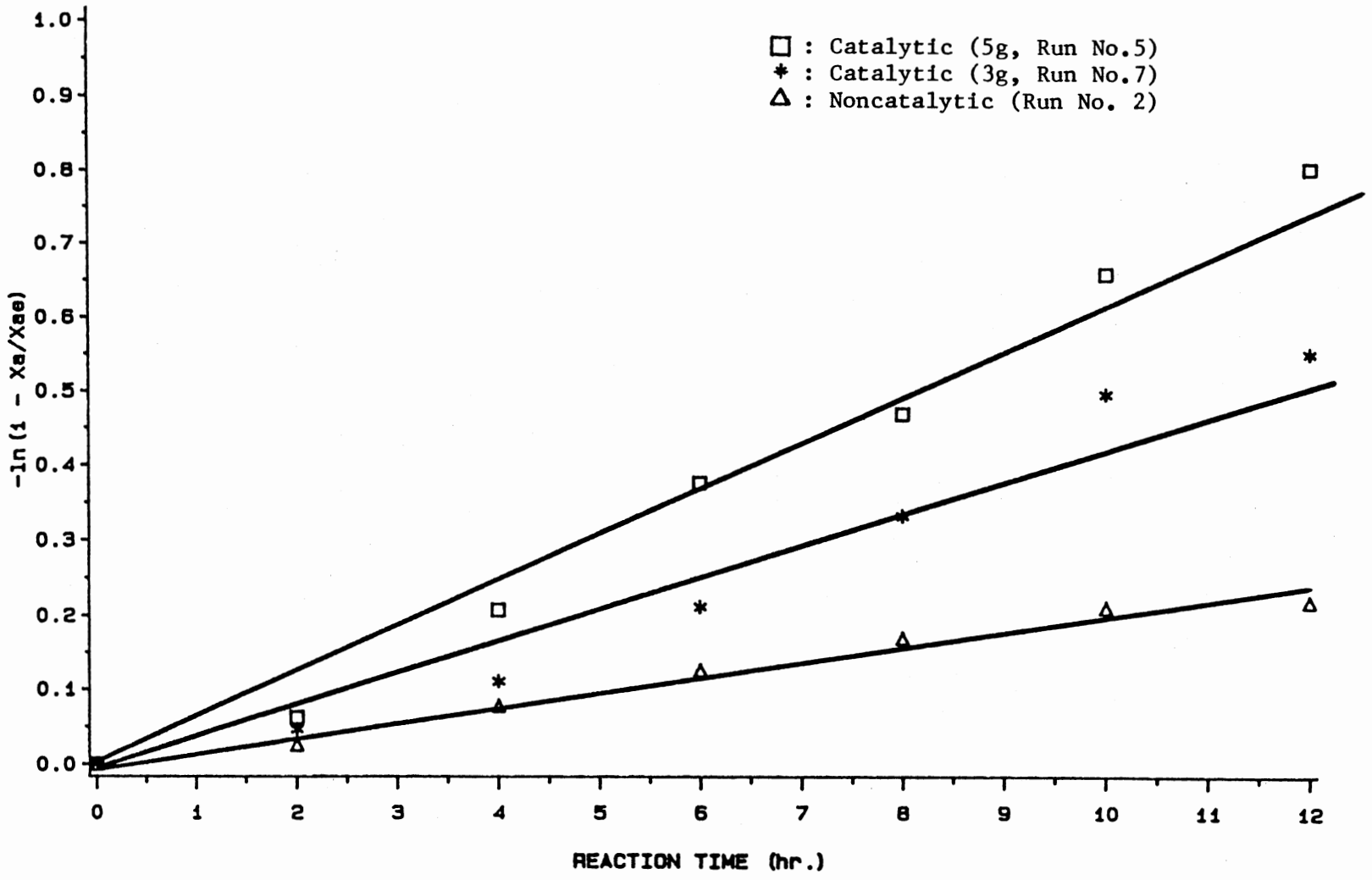

Figure 12. -ln(1-Xa/Xae) versus Time at 300 C
(Run No. 2, 5, and 7)

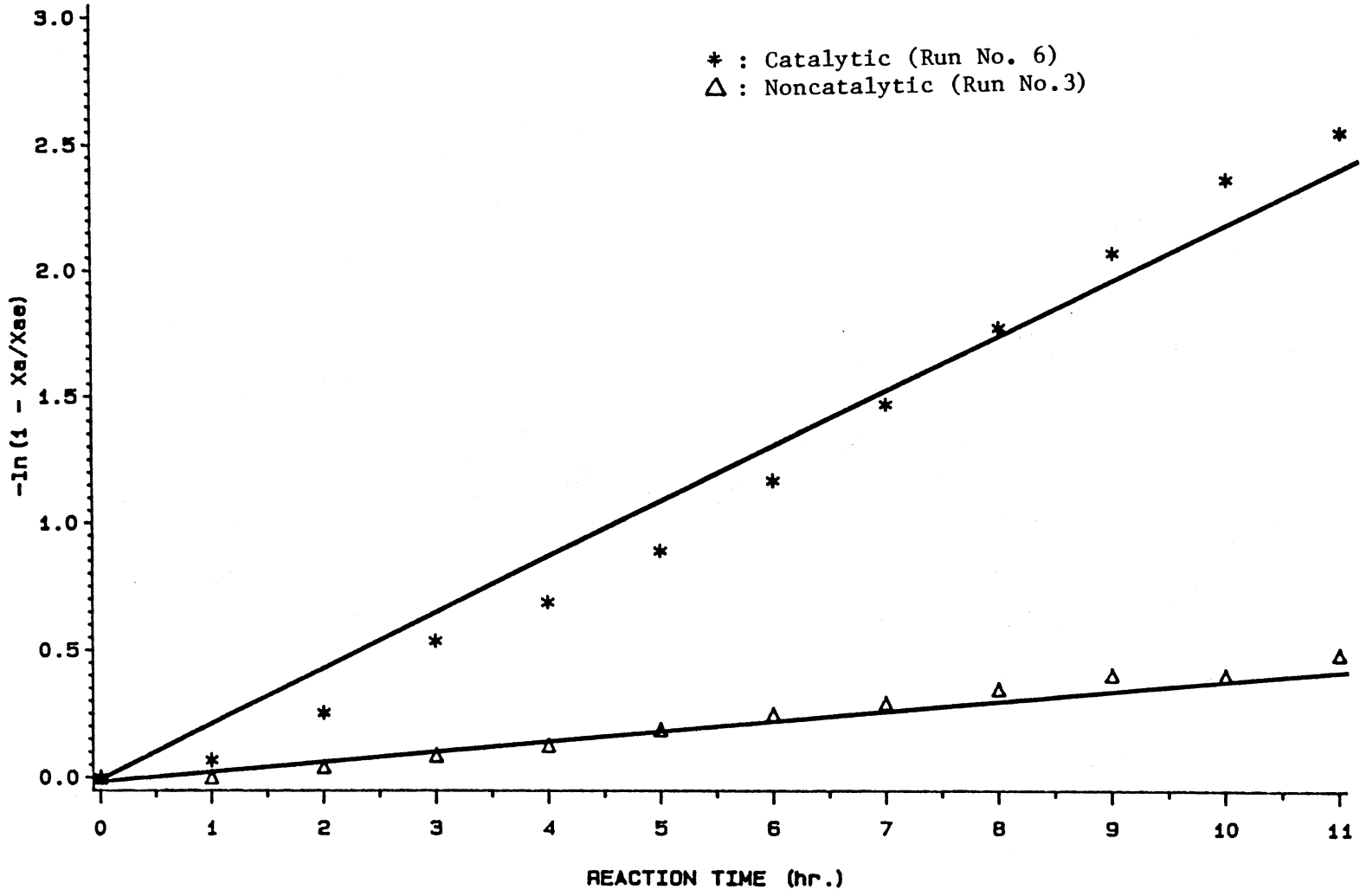

Figure 13. -ln(1-Xa/Xae) versus Time at 330 C
(Run No. 3 and 6)

TABLE XII

NONCATALYTIC REACTION RATE CONSTANTS [a]
BY PSEUDO-FIRST ORDER MODEL

Temp.(°C)	k'	k_2
270	1.10E-3 ± 4.96E-5	2.21E-6 ± 9.94E-8
300	2.04E-2 ± 3.84E-4	1.23E-4 ± 2.32E-6
330	4.05E-2 ± 1.56E-3	7.83E-4 ± 3.02E-5

a. Unit of rate constant = 1 / hr.

TABLE XIII

CATALYTIC[a] REACTION RATE CONSTANT[b]
BY PSEUDO-FIRST ORDER MODEL

Temp.(°C)	k'	k_2
270	1.31E-2 ± 8.32E-4	2.62E-5 ± 1.67E-6
300	6.18E-2 ± 2.97E-3	3.73E-4 ± 1.79E-5
330	1.97E-1 ± 1.29E-2	3.81E-3 ± 2.50E-4

a. Unit of rate constant = 1 / hr.
b. Amount of catalyst = 5 g

TABLE XIV

RESULTS OF PSEUDO-FIRST ORDER KINETIC MODEL AT 270 °C*

Amount of Cat. (g)	Time (hr.)	Actual Conv.	Predicted Conv.	Percentage** Rel. Dev.(%)
0	1	0.001	0.001	0
	2	0.001	0.002	-100
	3	0.003	0.003	0
	4	0.004	0.004	0
	5	0.003	0.006	-100
	6	0.007	0.007	0
	7	0.008	0.008	0
	8	0.010	0.009	10
	9	0.010	0.010	0
	10	0.012	0.011	8.33
	11	0.013	0.012	8.33
5	1	0.022	0.013	40.91
	2	0.050	0.026	47.27
	3	0.067	0.039	42.73
	4	0.072	0.051	29.23
	5	0.080	0.063	20.86
	6	0.088	0.076	13.85
	7	0.095	0.088	7.37
	8	0.099	0.099	-0.86
	9	0.099	0.111	-13.88
	10	0.108	0.123	-13.62
	11	0.116	0.134	-15.18

* Equilibrium conversion at 270 °C, X_{Ae} = 0.998

** Percentage relative deviation = (actual conv.-predicted conv.) / actual conv. * 100

TABLE XV

RESULTS OF PSEUDO-FIRST ORDER KINETIC MODEL AT 300 °C*

Amount of Cat. (g)	Time (hr.)	Actual Conv.	Predicted Conv.	Percentage Rel. Dev.(%)
0	1	0.010	0.020	-103.36
	2	0.025	0.040	-58.93
	3	0.055	0.059	-7.59
	4	0.074	0.078	-6.60
	5	0.095	0.097	-1.84
	6	0.116	0.115	0.86
	7	0.135	0.133	1.75
	8	0.154	0.150	2.13
	9	0.178	0.167	6.11
	10	0.187	0.184	1.64
	11	0.193	0.200	-3.82
3	1	0.028	0.041	-45.02
	2	0.045	0.080	-80.40
	3	0.075	0.118	-56.81
	4	0.103	0.154	-49.76
	5	0.136	0.189	-39.03
	6	0.188	0.222	-18.20
	7	0.238	0.254	-6.91
	8	0.279	0.285	-2.00
	9	0.327	0.314	3.84
	10	0.387	0.342	11.51
	11	0.414	0.369	10.88
	12	0.419	0.395	5.76
5	2	0.059	0.116	-96.56
	4	0.185	0.218	-17.99
	6	0.310	0.308	0.77
	8	0.370	0.386	-4.30
	10	0.477	0.456	4.42
	12	0.545	0.517	5.13

* Equilibrium conversion at 300 °C, XAe = 0.994

TABLE XVI

RESULTS OF PSEUDO-FIRST ORDER KINETIC MODEL AT 330 oC *

Amount of Cat. (g)	Time (hr.)	Actual Conv.	Predicted Conv.	Percentage Rel.Dev.(%)
0	1	0.002	0.040	-2617.45
	2	0.040	0.078	-93.83
	3	0.081	0.113	-40.22
	4	0.116	0.149	-28.71
	5	0.167	0.182	-9.25
	6	0.214	0.214	0.16
	7	0.248	0.246	1.24
	8	0.287	0.274	4.55
	9	0.325	0.302	7.11
	10	0.324	0.329	-1.53
	11	0.378	0.355	6.08
5	1	0.065	0.177	-172.70
	2	0.219	0.320	-46.05
	3	0.408	0.437	-7.13
	4	0.488	0.531	-8.77
	5	0.578	0.608	-5.06
	6	0.677	0.670	1.02
	7	0.757	0.721	4.71
	8	0.817	0.762	6.71
	9	0.860	0.796	7.47
	10	0.891	0.823	7.67
	11	0.907	0.845	6.81

* Equilibrium conversion at 330 oC, X_{Ae} = 0.981

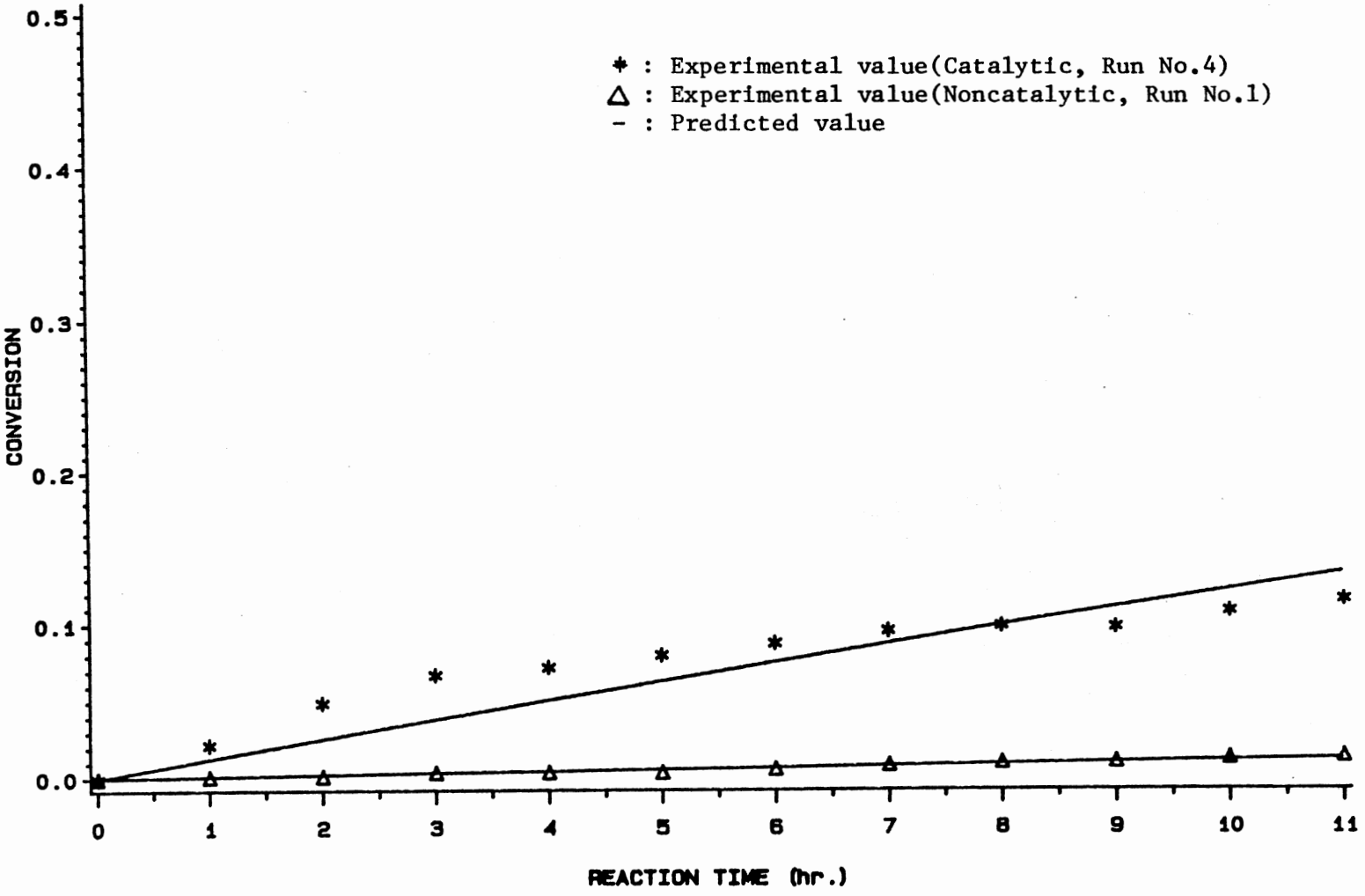

Figure 14. First Order Reversible Reaction Model for Quinoline Hydrogenation at 270 C

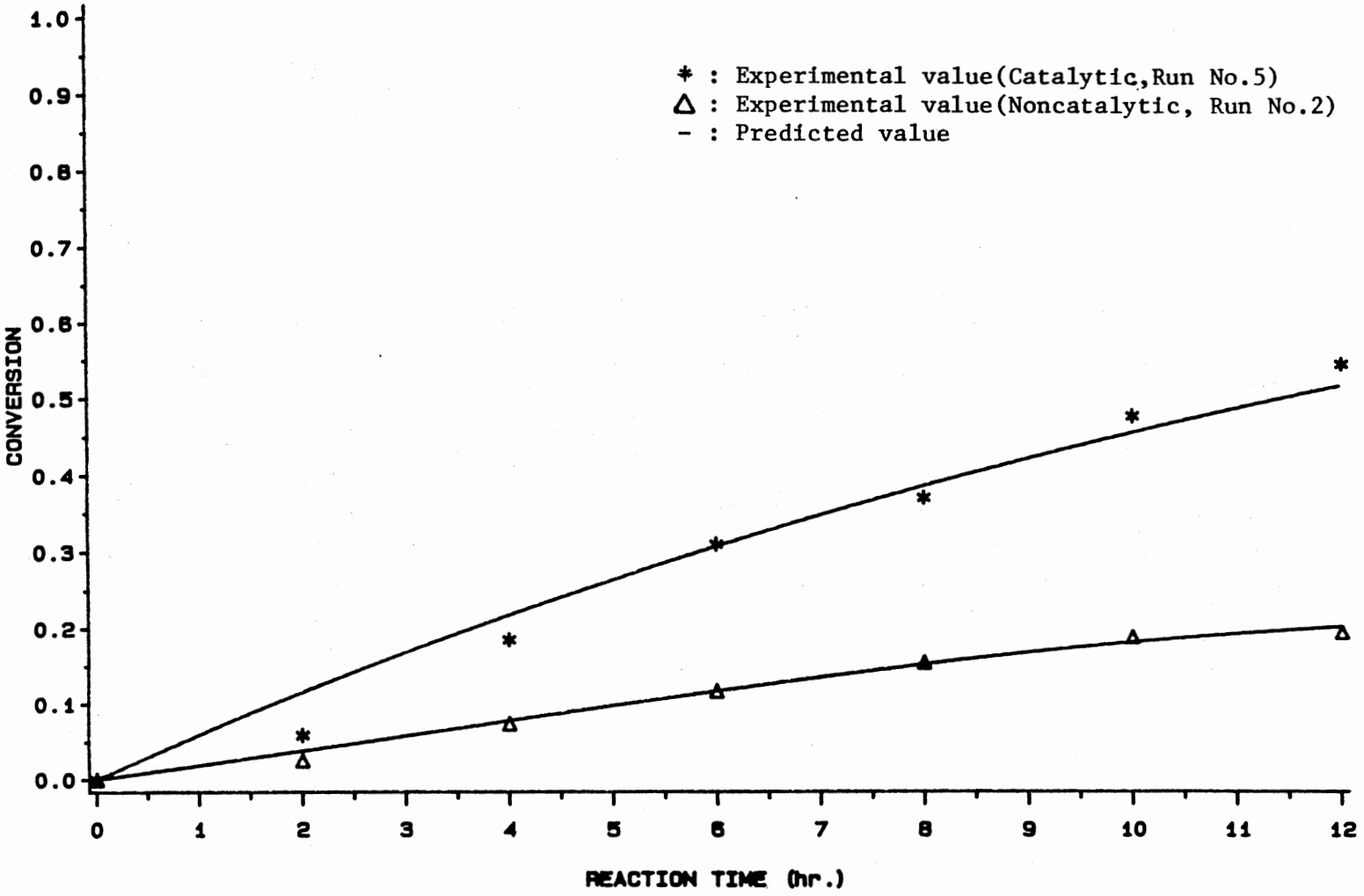

Figure 15. First Order Reversible Reaction Model for Quinoline Hydrogenation at 300 C

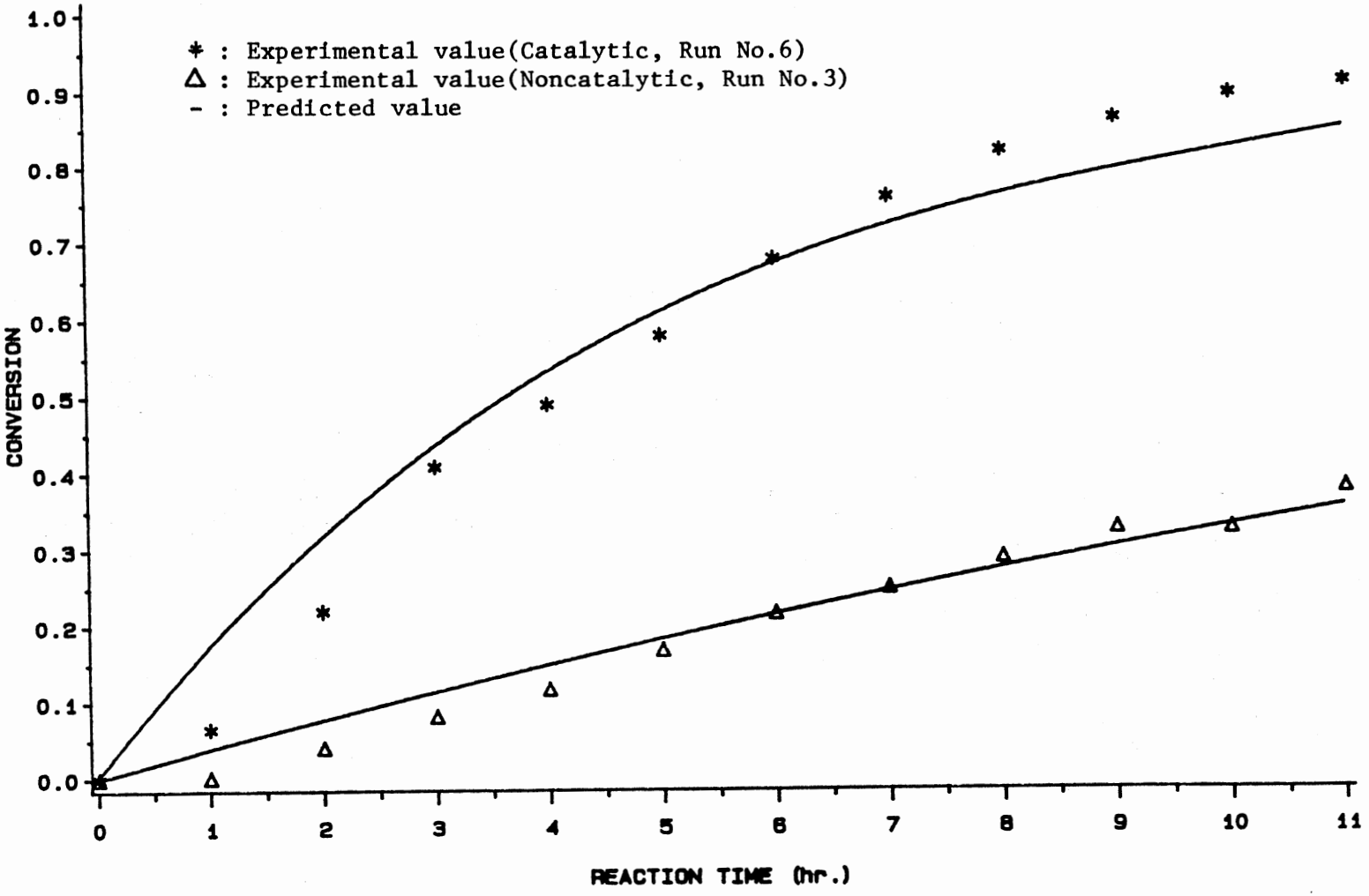

Figure 16. First Order Reversible Reaction Model for Quinoline Hydrogenation at 330 C

means that molybdenum nitride has a positive catalytic effect on the hydrogenation of quinoline. In order to make a meaningful evaluation of the catalytic properties of molybdenum nitride, the rate constants obtained from this project should be compared with those obtained from the previous works at which the sulfided commercial catalysts were used. Cocchetto, et al. (1981), Yang, et al. (1983), and Lee (1988) estimated the rate constants of the conversion reaction of quinoline to Py-THQ by different ways and it is impossible to compare their results with those of this work because they have different units.

Aboul-Gheit (1975) and Shih (1977) also reported the rate constants of each step in the quinoline HDN network except that of the first hydrogenation step in which quinoline is hydrogenated to Py-THQ. The rate constant of the hydrogenation of quinoline was too large to be measured compared with those of the rest of the reactions. They reported that the hydrogenolysis step, where Py-THQ is converted into o-propylaniline (OPA), had the smallest value of the rate constant among all steps in HDN network. Comparing the value of k' of this work with the rate constants of different steps which are reported by them, the catalytic performance of molybdenum nitride can be indirectly compared with those of the presulfided HDN catalysts.

The rate constants in the present catalytic reactions were recalulated to make them be independent on the weight of the catalyst, and are shown in Table XVII. Then the

TABLE XVII

CATALYTIC REACTION RATE CONSTANTS[a]
ON THE BASIS OF WEIGHT

Temp.(°C)	k'	k_2
270	2.62E-3 ± 1.66E-4	5.26E-6 ± 3.34E-7
300	1.24E-2 ± 5.94E-4	7.46E-5 ± 3.58E-6
330	3.94E-2 ± 2.58E-3	7.62E-4 ± 5.00E-5

a. Unit of rate constant = 1 / (g cat. hr)

value of k' was estimated at 350 °C by using the three values of k' at three different temperatures of 270, 300, 330 °C. This value was compared with the data of Aboul-Gheit (1975) and Shih (1977) which are shown in Table XVIII. At 350 °C, the value of k' for molybdenum nitride is smaller than the smallest rate value, k_4, reported for the steps in quinoline HDN network. Therefore, if the values of k_1 were available in the other two works, it is obvious that the value of k' would have been much smaller than those from any other work using the sulfided commercial HDN catalysts. This may lead to a conclusion that the catalytic activity of molybdenum nitride is very small when compared with those of the sulfided NiMo/alumina or CoMo/alumina on the equal weight basis. However, an interesting thing is that the surface area of molybdenum nitride used in this work is also very small. Therefore, the catalytic activities should be compared on the basis of equal surface area of the catalysts. As can be seen in Table XIX, the value of k' is comparable with those of k_i other than k_1 from Shih's work, even though it is still much smaller than the value of k_1.

The values of k' in both catalytic and noncatalytic reactions, obtained from the first order reversible reaction model, were used to calculate the activation energies by using Arrhenius equation. Values of ln(k') are plotted versus 1/T in Figure 17 and 18 which give the activation energies of 165 ± 53.3 kJ/mol (39.4 ± 12.8 kcal/mol) and 121 ± 7.74 kJ/mol (29.0 ± 1.85 kcal/mol) for noncatalytic

TABLE XVIII

COMPARISON OF RATE CONSTANTS[a] AT 350 °C
ON THE BASIS OF WEIGHT

Variable	This work	Aboul-Gheit (1975)	Shih (1977)
k_1[b]	0.0825	fast[c]	fast[c]
k_2[d]	*	29.376	3.60
k_3[e]	*	89.712	78.0
k_4[f]	*	*	2.10
Catalyst	Mo_2N + MoN	$CoMo/Al_2O_3$	$NiMo/Al_2O_3$

a. Units = 1 / (g cat. hr.)
b. Rate constant for quinoline to Py-THQ
c. Too large to be measured
d. Rate constant for Py-THQ to OPA
e. Rate constant for quinoline to Bz-THQ
f. Rate constant for OPA to NH_3 and hydrocarbons

* The author did not measure the value.

TABLE XIX

COMPARISON OF RATE CONSTANTS[a] AT 350 °C
ON THE BASIS OF SURFACE AREA OF CATALYST

Variable	This work	Aboul-Gheit (1975)	Shih (1977)
k_1	0.229	fast	fast
k_2	*	3.747	0.027
k_3	*	11.443	0.016
k_4	*	*	0.589
Surface Area (m^2/g cat.)	1.8	196	265

a. Units = 1 / (surface area * hr.)

* The authors did not measure the value.

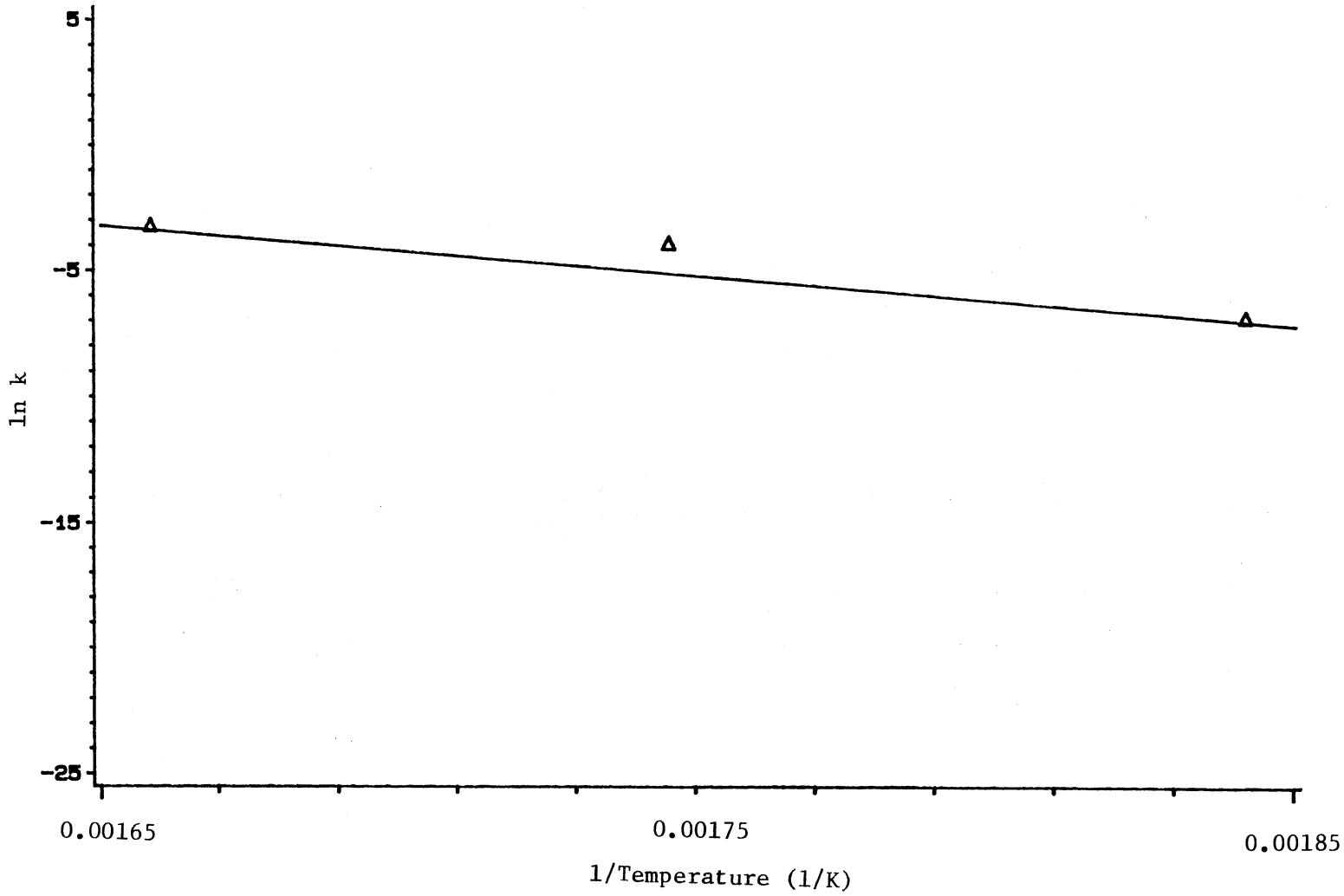

Figure 17. Arrhenius Plot of Quinoline Hydrogenation Data for Noncatalytic Reaction

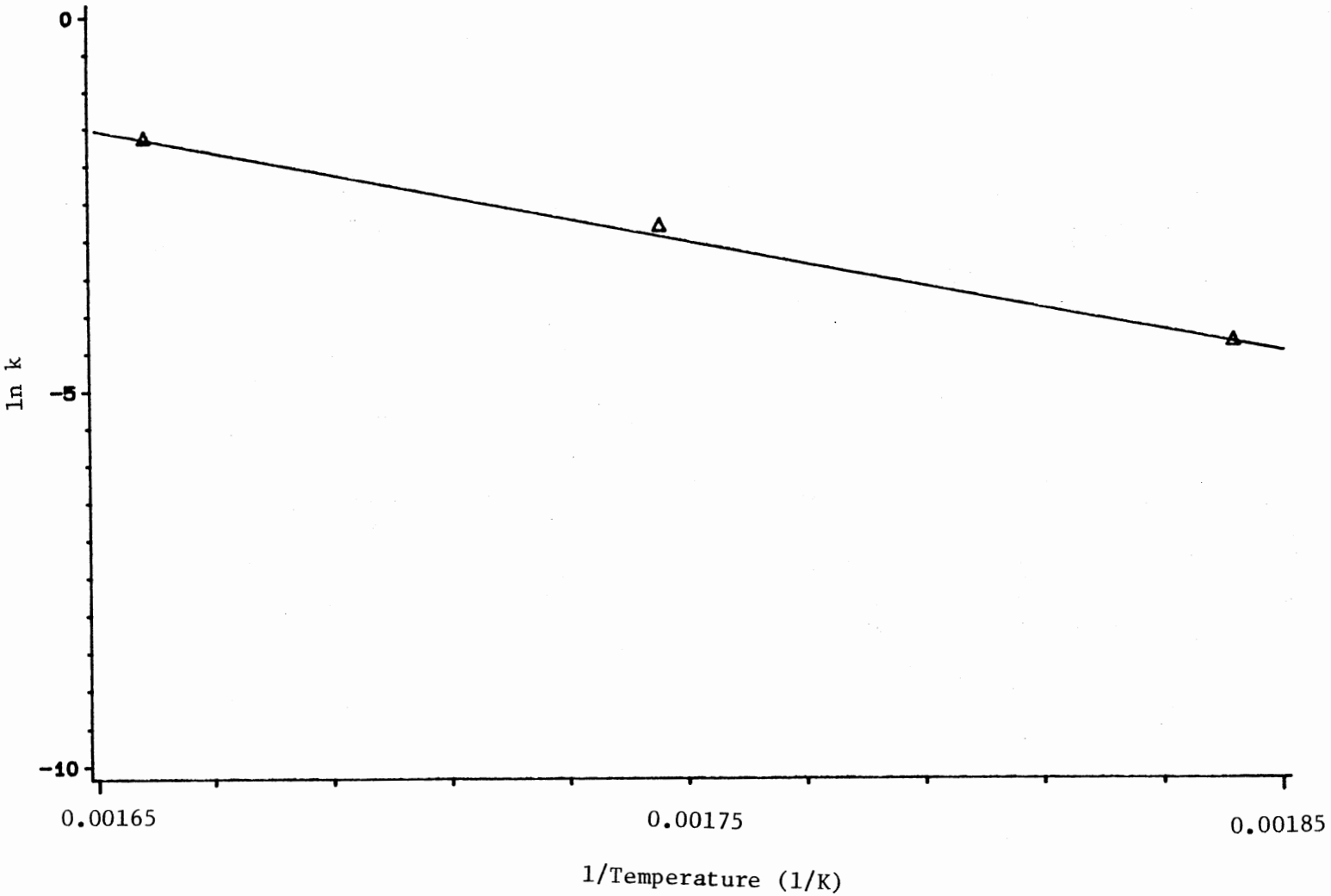

Figure 18. Arrhenius Plot of Quinoline Hydrogenation Data for Catalytic Reaction

and catalytic reactions, respectively. Then the rate constants of catalytic and noncatalytic reactions can be predicted by the following equation.

$$k'_{catalytic} = 6.21E09\ EXP(-14,600/T) \quad (8)$$

$$k'_{noncatalytic} = 1.15E13\ EXP(-19,900/T) \quad (9)$$

where T is the temperature in K. No published data about the activation energy of the hydrogenation of quinoline to Py-THQ is available. Even those authors who reported the rate constants of this step failed to obtain an accurate activation energy because the rate constants of this step were relatively inaccurate although the ratio of the forward rate constant to the backward rate constant could be accurately determined.

Introduction of molybdenum nitride into the reaction results in a reduction of activation energy by 44 kJ/mol (10 kcal/mol) or 27 % of the activation energy of the noncatalytic reaction, which clearly states the catalytic nature of the molybdenum nitride. While this catalytic activity is uniquely selective toward formation of Py-THQ, the inability of molybdenum nitride to carry out a denitrogenation reaction make it practically invaluable for HDN processes.

Langmuir-Hinshelwood Model

In this model the overall hydrogenation reaction was

assumed as;

$$A + 2H_2 \rightleftharpoons B \qquad (1)$$

where A is quinoline and B is Py-THQ. It was assumed that hydrogen was adsorbed on one type of site in atomic form, while quinoline adsorbed on a different site. The reaction occurred between the adsorbed hydrogen and quinoline. The product of the reaction was also adsorbed on the quinoline sites. Thus the mechanism of the reaction can be described as follows;

$$A + l \rightleftharpoons Al \qquad (10)$$

$$H_2 + 2m \rightleftharpoons 2Hm \qquad (11)$$

$$Al + Hm \rightleftharpoons AHl + m \qquad (12)$$

$$AHl + Hm \rightleftharpoons AH_2l + m \qquad (13)$$

$$AH_2l + Hm \rightleftharpoons AH_3l + m \qquad (14)$$

$$AH_3l + Hm \rightleftharpoons Bl + m \qquad (15)$$

$$Bl \rightleftharpoons B + l \qquad (16)$$

where l and m represent the adsorption sites for quinoline and hydrogen respectively. Assuming that reactions (13), (14), and (15) are very fast, concentraions of AHl, AH_2l, and AH_3l can be negligible compared with those of A_l and B_l.

Assuming reaction (12) and the backward reaction of reaction

(15) to be slow, the net controlling reaction rate can be written as;

$$r = r_{12} + r_{15} = k_{12}\, C_{A1}\, C_{Hm} - k_{15}'\, C_{B1}\, C_m \qquad (17)$$

where $CA_1 = K_{10}\, C_A\, C_1$,

$CB_1 = K_{16}\, C_B\, C_1$,

$C_{Hm} = (K_{11}\, C_{H2})^{0.5}\, C_m$

where r_{12} is the rate of forward reaction of reaction (12) and r_{15} is the rate of backward reaction of reaction (15), k_{12} is the forward rate constant of the reaction (12), k_{15}' is the backward rate constant of the reaction (15), C_i is the concentration of compound i, and C_1 and C_m are the concentrations of the sites 1 and m, respectively. The final rate equation is as below;

$$r = \frac{C_{tm}C_{t1}\,(k_{12}K_{10}K_{11}^{0.5}C_AC_{H2}^{0.5} - k_{15}'K_{16}C_B)}{(1 + K_{10}C_A + K_{16}C_B)\,(1+K_{11}^{0.5}C_{H2}^{0.5})} \qquad (18)$$

where K_j is the adsorption equilibrium constant in the reaction j, and C_{tm} and C_{t1} are the total concentrations of catalytic sites for hydrogen and nitrogen compounds respectively. Since the concentration of hydrogen is maintained constant, equation (14) can be rewritten as follows;

$$r = \frac{kK_{10}K_{11}' (C_A - C_B/K)}{(1 + K_{10}C_A + K_{16}C_B)} \qquad (19)$$

where

$$k = \frac{k_{12}C_{tm}C_{t1}}{(1 + K_{11}^{0.5}C_{H2}^{0.5})},$$

$$K = \frac{K_{10}K_{11}'K_{25}}{K_{16}}, \quad K_{11}' = K_{11}^{0.5}C_{H2}^{0.5},$$

$$\text{and } K_{25} = \frac{k_{12}}{k_{15}'}$$

In order to make a meaningful data for catalytic reactions, the amounts of Py-THQ produced by noncatalytic reactions were subtracted from those produced by catalytic reactions. A details of this calculation procedure is shown in Appendix C.

The least square method was used to get the best estimation for the model parameters. The results are presented in Tables XX and XXI. Percentage relative deviations in Table XXI indicates that this model does not fit the experimental data satisfactorily. No further work was done with this model.

If the adsorption of quinoline and Py-THQ on the catalyst are assumed to be weak, the denominator of equation

TABLE XX

PARAMETERS OF LANGMUIR-HINSHELWOOD KINETIC MODEL

Parameters	270 °C	300 °C	330 °C
K	1.0E-1	2.0E-1	1.0E-1
K_{10}	2.0E03	2.0E03	2.0E03
K_{11}'	3.0E03	3.0E03	4.0E03
K_{16}	2.0E03	2.0E03	1.0E03
k	1.0E-2	1.0E-2	2.0E-2

TABLE XXI

RESULTS OF LANGMUIR-HINSHELWOOD KINETIC MODEL

Temp. (°C)	Time (hr.)	Actual Conv. of THQ	Predicted Conv. of THQ	Percentage Rel.Dev.(%)
270	0	0.0000	0.0111	-
(Run No.	1	0.0009	0.0065	-597.66
4)	2	0.0029	0.0058	-98.27
	3	0.0038	0.0060	-59.07
	4	0.0047	0.0063	-32.78
	5	0.0057	0.0064	-11.39
	6	0.0056	0.0063	-13.29
	7	0.0060	0.0062	-3.33
	8	0.0052	0.0058	-10.53
	9	0.0051	0.0060	-16.60
	10	0.0068	0.0069	-1.83
	11	0.0067	0.0062	7.8
300	0	0.0000	0.0117	-
(Run No.	2	0.0022	0.0061	-172.38
5)	4	0.0063	0.0043	31.68
	6	0.0127	0.0040	68.60
	8	0.0136	0.0033	75.67
	10	0.0155	0.0023	85.20
	12	0.0202	0.0021	89.62
330	0	0.0000	0.0144	-
(Run No.	1	0.0082	0.0121	-47.99
6)	2	0.0212	0.0089	58.05
	3	0.0324	0.0054	83.32
	4	0.0355	0.0043	87.90
	5	0.0405	0.0035	91.37
	6	0.0506	0.0028	94.47
	7	0.0610	0.0022	96.39
	8	0.0711	0.0018	97.47
	9	0.0761	0.0013	98.29
	10	0.0879	0.0011	98.75
	11	0.0870	0.0010	98.85

(19) becomes almost equal to unity. Thus equation (19) can be expressed as;

$$r_{12} = k_1 C_A - k_2 C_B \qquad (20)$$

where

$k_1 = kK_{10}K_{11}'$ and $k_2 = kK_{10}K_{11}'/K$

Equation (20) is the same as equation (3) which fits the experimental data better than equation (19). It can be therefore said that the reaction may occur mainly between adsorbed hydrogen atoms and the weakly adsorbed quinoline molecules.

Catalyst Analysis

As shown in Table VII in Chapter IV, it was found that the weights of the used catalysts after burning at 550 °C for 60 hours increased unexpectedly. The averages of the weight increase of the fresh catalyst and the used catalyst were 0.375 and 0.37 g/g catalyst before burning, respectively. If it is assumed that molybdenum nitride (Mo_2N+MoN) is oxidized to molybdenum oxide (MoO_3), the weight should increase by the amount of 0.37 g/(g molybdenum nitride) which clearly matches the weight change of the catalyst. Furthermore the catalyst changed color from black to yellow green which agrees with the colors of molybdenum nitride and oxide respectively. Molybdenum nitride is usually obtained by reduction of molybdenum oxides in an atmosphere of nitrogen-

containing gases at temperatures above 1000 °C. These facts indicate that molybdenum nitride is oxidized to molybdenum oxide during the combustion. Because of this weight gain, the amount of coke deposited on the surface of the catalyst during the reaction could not be determined.

Combustion of the catalyst was also found to cause changes in the physical properties of the catalyst as can be seen in Table VIII. The surface area of the fresh catalyst increases by a factor of nine during the burning process. Meanwhile the increase of the pore volume is very small. However, in the used catalyst, increase of the surface area is so small that it can be negligible, compared with that of the fresh catalyst. The pore volume of the spent catalyst increases by a factor of two during burning. These data indicate that the reaction condition affects the physical properties of the catalyst. These effects were identified by Scanning Electron Microscopy (SEM) which are shown in Figures 19 - 23. Figures 19 and 21 were taken at a magnification of 400 from the fresh catalyst before and after burning, respectively. From these figures, it can be observed that the catalyst consisted of large crystals with small particles attached onto them. Figure 20, at a magnification of 4400, shows the small particles attached to the crystals. From this figure, the small particles appear to consist of a cluster of smaller crystals. By Energy Dispersion Spectrometer (EDS), these materials were identified as metallic molybdenum. The small surface area of the catalyst

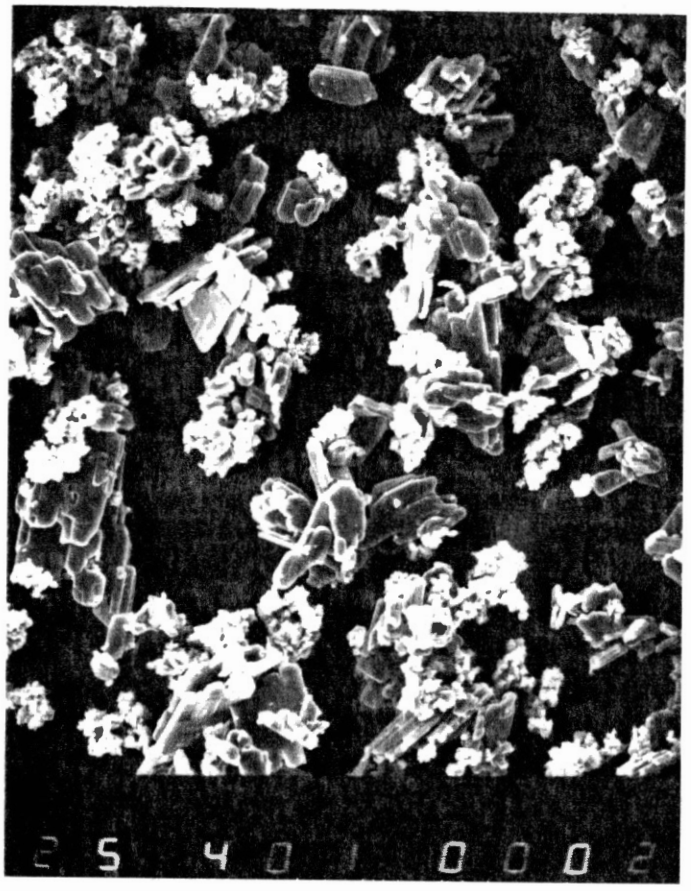

Figure 19. Result of SEM Analysis of Fresh Catalyst Before Burning at 550 C (X 400)

Figure 20. Result of SEM Analysis of Fresh Catalyst Before Burning at 550 C (X 4400)

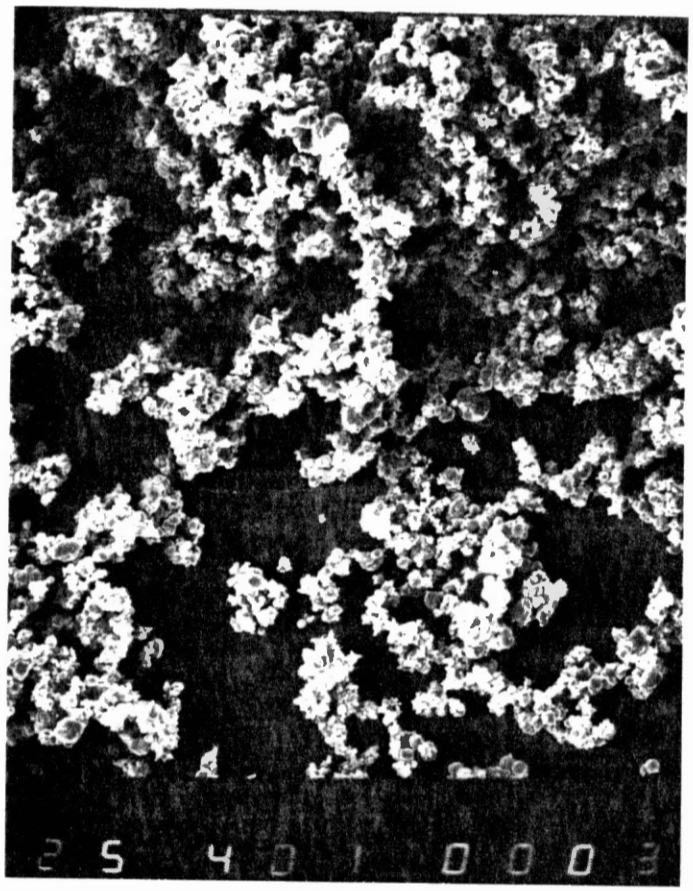

Figure 21. Result of SEM Analysis of Fresh Catalyst After Burning at 550 C (X 400)

Figure 22. Result of SEM Analysis of Used Catalyst Before Burning at 550 C (X 500)

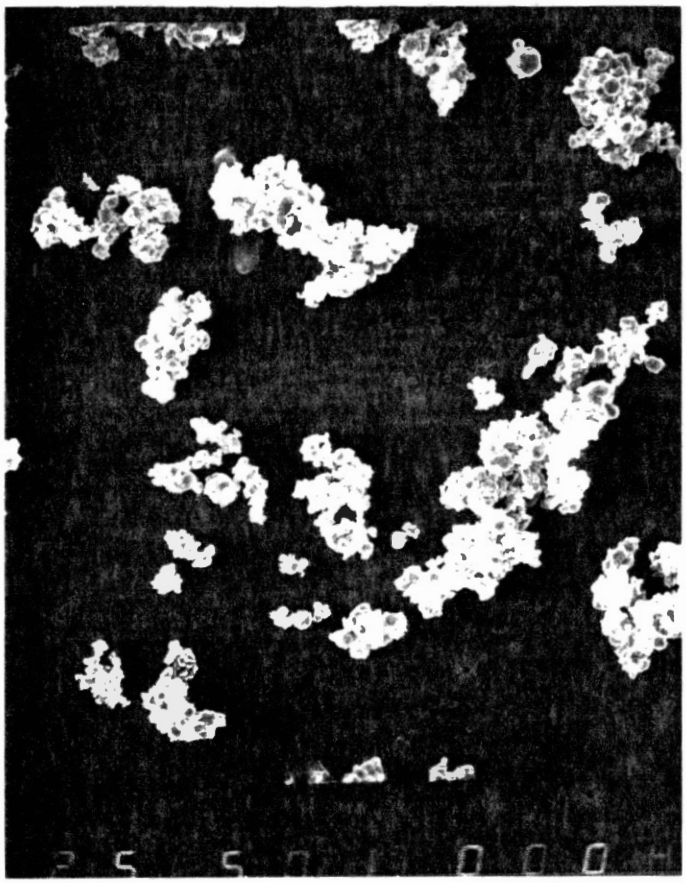

Figure 23. Result of SEM Analysis of Used Catalyst After Burning at 550 C (X 500)

is due to the non-porous crystalline structure of these particles.

Figure 21 shows a micrograph of the fresh catalyst after burning. The large crystals are broken into small pieces which have large surface areas. It is expected that the crystals swelled by the released nitrogen at high temperatures and then popped like a pop-corn. These changes of the crystals in the fresh catalyst caused the increase in the surface area of the catalyst after burning.

Figure 22 and 23, at a magnification of 500, show micrographs of the catalysts used at 300 °C (Run No. 5), before and after burning. Compared with the fresh catalyst before burning, the used catalyst, which has been exposed to gradual increase of temperature from room temperature to the reaction temperature, has different shape particles. The large crystals of the fresh catalyst are broken into the small pieces slowly during the reaction, causing an increase in the surface area of the catalyst. By burning, the shapes of the particles are changed, as seen in Figure 23, without a significant increase in the surface area. The large crystals develop cracks and somewhat lose their mechanical compactness during the reaction. Therefore in the burning process, the released nitrogen escapes from inside the crystals without popping the crystals. Because of the differences in their aging history, the fresh and used catalysts respond differently to the burning process.

CHAPTER VI

CONCLUSIONS AND RECOMMENDATIONS

In this work, the hydrogenation of quinoline was investigated over molybdenum nitride powder as the catalyst. The catalytic properties of the catalyst were evaluated and compared with those of the presulfided commercial catalysts. A model for the hydrogenation of quinoline was developed. From this study, the following conclusions are drawn;

1. The hydrogenation of quinoline over molybdenum nitride as well as noncatalytic reactions was found to produce only Py-THQ with no by-products under the reaction conditions studied.

2. The formation of Py-THQ was favored by increasing temperatures in the ranges of the reaction temperatures. The amount of Py-THQ producted during the reaction increased with the amount of the catalyst. The conversion rate of quinoline to Py-THQ was found to be slow and that the reaction could not attain its chemical equilibrium state within the duration of the experiment.

3. A pseudo-first order reversible kinetic model fits the experimental data well. The rate constants obtained from this model were found to be very small compared with those from reactions over presulfided molybdenum based

catalysts. Molybdenum nitride was considered to have a specific selectivity in quinoline hydrogenation with no HDN activity. Meanwhile it has a very low activity, in contrast to the commercial HDN catalysts.

4. The physical properties of molybdenum nitride used in this project were found to be changed by the atmosphere of the reaction. Combustion of molybdenum nitride at a high temperature to analyse the coke content causes the oxidation of the catalyst to form molybdenum oxide.

The following recommendations are made for further investigations:

1. An investigation of quinoline hydrogenation over molybdenum nitride at higher temperature should be performed to verify the selectivity of molybdenum nitride at higher temperatures.

2. DHQ can be used as a feed to investigate the catalytic properties of molybdenum nitride further. This catalyst is considered to have hydrogenolysis sites. The conversion of DHQ to PBZ is known to be as fast as that of quinoline to Py-THQ. Therefore, to use the saturated compound as a feed is useful to identify the real hydrogenolysis properties. If it shows an ability to break the carbon-nitrogen bond, it will become feasible to study the HDN activity of molybdenum nitride with oils.

3. To identify the role of the nitrogen atoms in the molybdenum nitride, pure molybdenum should be used as a catalyst and the result compared with that of this work.

REFERENCES

Aboul-Gheit, A. K., "The Kinetics of Quinoline Hydrodenitrogenation through Reaction Intermediate Products," Can. J. Chem., 53, 2575 (1975)

Aboul-Gheit, A. K. and Abdou, I. K., "The Hydrogenation of Petroleum-Model-Nitrogen Compounds," J. Inst. Petrol. London, 59, 188 (1973)

Aika, K. and Ozaki, A., "Mechanism and Isotope Effect in Ammonia Synthesis over Molybdenum Nitride," J. of Cat., 14, 311 (1969)

Bergstrom, F. W. and Carson, J. F., "Alkali and Alkaline Earth Metals as Catalysts in the Hydrogenation of Organic Compounds," Amer. Chem. Soc. J., 63, 2934 (1941)

Bhinde, M. V., "Quinoline Hydrodenitrogenation Kinetics and Reaction Inhibition," Ph.D. Dissertation, University of Delaware, Delaware (1979)

Boudart, M., Dyama, S. T., and Leclercq, L., "Molybdenum Carbide, Oxycarbide, and Nitride as Catalysts in the Activation of C-O, N-N, C-C, and H-H Bonds," Proc. 7th Inc. Cong. Catalysis, (Seiyama, T. and Tanabe, K., Eds), Elsevier, Amsterdam, vol 1, 578 (1980)

Cocchetto, J. F. and Satterfield, C. N., "Thermodynamic Equilibria of Selected Heterocyclic Nitrogen Compounds with Their Hydrogenated Derivatives," Ind. Eng. Chem. Process Des. Dev., 15, 272 (1976)

Cocchetto, J. F. and Satterfield, C. N., "Chemical Equilibria among Quinoline and Its Reaction Products in Hydrodenitrogenation," Ind. Eng. Chem. Process Des. Dev., 20, 49 (1981)

Curtis, C. W. and Caheal, D. R., "Hydrodenitrogenation of Quinoline and Coal Using Transition Metal Sulfides," Preprint, Div. Fuel Chem., ACS, 32(3), 315 (1987)

Diworky, F. F. and Adkins, H., "Competitive Hydrogenations. II," Amer. Chem. Soc. J., 53, 1868 (1931)

Doelman, J. and Vulgter, J. C., "Proceedings, Sixth World

Petroleum Congress," Section III, pp 247-257, The Hague, Netherlands (1963)

El-Bishtawi, R. F., "Hydrodenitrogenation of Quinoline, Acridine, and Their Mixture," Ph.D. Dissertation, Okla. St. Univ., Stillwater, OK. (1986)

Eru, I. I., Lange, A. A., Zeidlitz, E. M., and Strel'nikova, V. P., "The Catalytic Hydrogenation of Quinoline to Kusol," Chem. Abs., 58, 6785 (1963)

Fish, R. H., Tan, J. L., and Thormodsen, A. D., "Homogeneous Catalytic Hydrogenation. 2. Selective Reduction of Polynuclear Heteroaromatic Compounds Catalyzed by Chlorotris (triphenylphosphine) rhodium (I)," J. Org. Chem., 49, 4500 (1984)

Flinn, R. A., Larson, O. A., and Beuther, H., "How easy is Hydrodenitrogenation ?," Hydrocarbon Process. Petrol. Refiner, 42(9), 129 (1963)

Glora, F. and Lee, V., "Effect of Hydrogen Pressure on Catalytic Hydrodenitrogenation of Quinoline," Ind. Eng. Chem. Process Des. Dev., 25, 918 (1986)

Haddix, G. W., Reimer, J. A., and Bell, A. T., "Characterization of Hydrogen Adsorbed on Molybdenum Nitride by NMR Spectroscopy," J. of Cat., 108, 50 (1987)

Ipatiev, W., "Quinoline, Part I," (Gurnos, J., Eds), John Wiley and Sons, 27 (1977)

Leary, K. J., Michaels, J. N., and Stacy, A. M., "Carbon and Oxygen Atom Mobility during Activation of Molybdenum Carbide Catalysts," J. of Cat., 101, 301 (1986)

Lee, Y. N., "Adsorption and Kinetic Studies of Quinoline Hydrodenitrogenation and its Intermediate Compounds," Ph.D. Dissertation, Okla. St. Univ., Stillwater, OK. (1988)

Levy, R. B., "Advanced Materials in Catalysis," Academic Press, New York, 101 (1971)

Levy, R. B. and Boudart, M., "Platinum-Like Behavior of Tungsten Carbone Monoxide on Surface Catalysis," Science, 181, 547 (1973)

Logan, M., Gellman, A., and Somorjai, G. A., "Hydrogenation of Carbon Monoxide on Mo(100) Single Crystal and Polycrystalline Foils," J. of Cat., 94, 60 (1985)

Nakhmanovich, A. S. and Kalechits, I. V., "Liquid Phase

Hydrogenation of Polycyclic Hydrocarbons and Heterocyclic Compounds over Pt Catalyst," Chem. Abs., 60, 10497 (1964)

Oyama, S. T. and Haller, G. L., "Catalysis," (Bond, G. C. and Webb, G., Eds), Specialist Periodical Reports, vol. 5, The Chemical Society, London, 333 (1981)

Palfray, L., "Quinoline, Part I," (Gurnos, J. Eds), John Wiley and Sons, 27 (1977)

Ponomarev, A. A. and Dyukareva, V. N., "Hydrogenation of Nitrogen Heterocycles on Ruthenium Catalyst," Chem. Abs., 78, 4101 (1973)

Ranhotra, G. S., Haddix, G. W., and Reimer, J. A., "Catalysis over Molybdenum Carbides and Nitrides, I. Catalyst Characterization," J. of Cat., 108, 24 (1987)

Roberti, G., "The Hydrogenation of Nitrogenous Compounds from Coal Tar," Chem. Abs., 26, 580 (1932)

Rollmann, L. D., "Catalytic Hydrogenation of Model Nitrogen, Sulfur, and Oxygen Compounds," J. of Cat., 46, 243 (1977)

Sabatier, A. and Murat, M., "Quinoline, Part I," (Gurnos, J., Eds), John Wiley and Sons, 27 (1977)

Saito, M. and Anderson, R. B., "The Activity of Several Molybdenum Compounds for the Methanation of CO," J. Cat., 63, 438 (1980)

Satterfiels, C. N. and Carter, D. L., "Effects of Water Vapor on the Catalytic Hydrodenitrogenation of Quinoline," Ind. Eng. Chem. Process Des. Dev., 20, 538 (1981)

Satterfield, C. N. and Cocchetto, J. F., "Reaction Network and Kinetics of the Vapor-Phase Catalytic Hydrodenitrogenation of Quinoline," Ind. Eng. Chem. Process Des. Dev., 20, 53 (1981)

Satterfield, C. N. and Gültekin, S., "Effect of Hydrogen Sulfide on the Catalytic Hydrodenitrogenation of Quinoline," Ind. Eng. Chem. Process Des. Dev., 20, 62 (1981)

Satterfield, C. N., Modell, M., Hites, R. A., and Declerck, C. J., "Intermediate Reactions in the Catalytic Hydrodenitrogenation of Quinoline," Ind. Eng. Chem. Process Des. Dev., 17, 141 (1978)

Satterfield, C. N., Modell, M., and Mayer, J. F., "Interactions between Catalytic Hydesulfuriation of Thiophene and Hydrodenitrogenation of Pyridine," AIChE J., 21-6, 1100 (1975)

Schrader, G. L. and Cheng, C. P., "In Situ Laser Raman Spectroscopy of the Sulfiding of Mo/Alumina Catalysts," J. of Cat., 80, 369 (1983)

Shih, S. S., Katzer, J. R., Kwart, H., and Stiles, A. B., "Quinoline Hydrodenitrogenation: Reaction Network and Kinetics," Preprints, Div. Petr. Chem., ACS, 919 (1977)

Shono, S., Itabashi, K., Yamada, M., and Kikuchi, M., "Catalytic Hydrogenation of Organic Compounds by Molybdenum Trisulfide," Chem. Abs., 58, 4390 (1963)

Sonnemans, J., and Mars, P., "The Mechanism of Pyridine Hydrogenolysis on Molybdenum-Containing Catalysts. I. The Monolayer MoO_3-Al_2O_3 Catalyst: Preparation and Catalytic Properties," J. of Cat., 31, 209 (1973)

Suarez, W., Dumesic, J. A., and Hill, C. G., "Acidic Properties of Molybdena-Alumina for Different Extents of Reduction: Infrared and Gravimetric Studies of Adsorbed Pyridine," J. of Cat., 94, 408 (1983)

Sultanov, A. S., Safaev, A, S., Arifdzhanov, A., Abdukadyrov, A., Rusmanova, M. M., and Akhundzhanov, A., "Methods for Analysing the Products of Some Catalytic Reactions," Chem. Abs., 68, 8990 (1968)

Svajgl, O., "Refining of Liquid Hydrocarbon Mixtures by Hydrogenation of Organic Nitrogen Bases," Chem. Abs., 80, 50194 (1974)

Toth, L. E., "Transition Metal Carbides and Nitrides," Academic Press, New York, (1971)

Volpe, L. and Boudart, M. J."Compounds of Molybdenum and Tungsten with High Specific Surface Area,", Solid State Chem., 59, 332, 348 (1985)

Volpe, L. and Boudart, M. J., "Ammonia Synthesis on Molybdenum Nitride," J. Phys. Chem., 90, 4874 (1986)

von Braun, J., Petzold, A., and Seeman, J., "Quinoline, Part I," (Gaurnos, J., Eds), John Wiley and Sons, 27 (1977)

Wedekind, E. and Maiser, G. L., "Quinoline, Part I," (Gurnos, J., Eds), John Wiley and Sons, 27 (1977)

Weiser, J., "1,2,3,4-tetrahydroquinoline from Coke-Chemical Products," Chem. Abs., 78, 4144 (1973)

Yang, S. H. and Satterfield, C. N., "Some Effects of Sulfiding of a NoMo/Alumina Catalyst on Its Activity for

Hydrodenitrogenation of Quinoline," J. of Cat., 81, 168 (1983)

Yang, S. H. and Satterfield, C. N., "Catalytic Hydrodenitrogenation of Quinoline in a Trickle-Bed Reactor. Effect of Hydrogen Sulfide," Ind. Eng. Chem. Process Des. Dev., 23, 20 (1984)

Yang, R. T. and Wong, C., "Catalysis of Carbon Oxidation by Transition Metal Carbide and Oxide," J. of Cat., 85, 154 (1984)

APPENDIXES

APPENDIX A

ANALYTICAL PROCEDURE

The analytical equipment to measure the concentrations of the reaction products was a Hewlett Packard Model 5890A Gas Chromatograph, equipped with a 60 m DB-1 capillary column and a thermal conductivity detector. The output of the detector was integrated and recorded by a Hewlett Packard Integrator Model 3392A. The chromatograph was programmed to obtain maximum separations between peaks in a reasonable time period. The column temperature was initially held at 60 °C for 2 minutes. Then the temperature was increased at 8 °C/min. rate until it reached 200 °C. The column was held at this temperature for at least 9 minutes. Approximately, 0.1 microliter of the liquid sample was injected into the GC through an injection port which was maintained at 225 °C to vaporize the injected sample. Helium used as the carrier gas was then mixed with the vaporized sample. Helium gas was delivered in chromatographic grade and was used without any further purification.

The compounds in the liquid samples were identified by comparing the retention times of the unknown peaks in chromatograms with retention times of the standard compounds. Physical properties and manufactures of the standard com-

pounds used to calibrate the chromatographic peaks are shown in Table XXII. By using known concentrations of each compound, the response factors were obtained. The response factors were used to estimate the weight percents of the compounds in the sample. Table XXIII shows the listing of the retention times along with the response factors for different compounds.

The accuracy of the gas chromatographic analyses was checked periodically throughout the experiments. This was done simply by injecting the same liquid samples three times successively and then selected peaks were compared to each other in terms of the compositions calculated. Table XXIV gives an example of such analysis. The calculated concentrations of quinoline and Py-THQ are very closed to each other. It can be seen that the maximum deviation from average is 3.78 percent. For all the GC analyses that the deviation was checked, this figure was not exceeded.

All of the GC analysis data that was gathered is available from this investigator or Dr. Seapan of School of Chemical Engineering at Oklahoma State University.

TABLE XXII

CHARACTERISTICS OF STANDARD COMPOUNDS

Compound	Molecular Weight	Boiling pt. (°C)	Purity* (%)	Manufacturer
Quinoline	129.16	237	99.99	Alfa Products
Py-THQ	133.19	249	98.00	Alfa Products
Bz-THQ	133.19	218	99.00	Alfa Products
n-Hexadecane	226.48	287	99.00	Alfa Products

* From vendor's data

TABLE XXIII

RETENTION TIMES AND RESPONSE FACTORS

Compound	Retention Time (min.)	Response Factors
Quinoline	17.85	1.484
Py-THQ	19.52	1.399
Bz-THQ	16.11	1.377
n-Hexadecane	27.40	1.000

TABLE XXIV

ACCURACY OF GC ANALYSIS*

Compound	Concentration (wt. %)	Deviation from avg.(%)	Standard Deviation
Quinoline	1.81	+ 2.16	
	1.92	- 3.78	
	1.83	+ 1.08	
			0.048
Py-THQ	3.12	+ 1.58	
	3.20	- 0.95	
	3.18	- 0.32	
			0.034

* Run No. 6 at 5 hr.

APPENDIX B

EXPERIMENTAL PROCEDURE

The experimental procedure consists of the following steps; purging and gas leakage checking, heating, changing gases, reaction, sampling, and shut down.

Purging and Gas Leak Checking

1. The catalyst and the liquid reactants are poured into the glass liner which is located in the reactor.

2. The cover is carefully placed on top of the reactor and tightened, while all the valves are closed.

3. Nitrogen gas is slowly introduced into the reactor through valves # 22 and 24 until the pressure reaches 1500 psig. The system is tested for any leaks. A pressure drop of less than 50 psig in an hour is considered acceptable.

Heating and Gas Changing

1. The set point of the temperature controller is raised to the temperature of about 80 ^{o}C higher than the reaction temperature. Then heating of the reactor is started while the reactor is kept under nitrogen pressure.

2. During the heating process, the pressure and

temperature are monitored by the pressure gauge and the digital indicator, respectively.

3. The heating process continues for 3 hours. When the desired reaction temperature is reached the valves # 22 and 24 are closed and the valves # 14 and 16 are slightly opened so that the pressure decreases to 1000 psig.

4. Then valves # 14 and 16 are closed and the system is pressurized to the reaction pressure by the introduction of hydrogen through the valves # 11, 12, and 20.

5. Steps 3 and 4 are repeated for ten times in about 30 minutes in order to ensure the removal of nitrogen from the reactor.

6. Finally, the system is pressurized by hydrogen. The valves # 11, 12, and 20 are left open during the reaction.

Reaction

1. The sample number zero is taken as soon as gas displacement is completed. This is considered as the starting point of the reaction.

2. The stirrer is started at a low speed and raised to 650 rpm. All valves except the valves # 11, 12, 15, and 20 are closed.

3. The cooling water is introduced into the cooling coil to prevent the system from overheating during the reaction.

Sampling

1. The stirrer is turned off.

2. Nitrogen is introduced into the sampling cylinder and trap through the valves # 23, 24, and 17 to pressurize the sampling system to about 1000 psig.

3. After closing the valves # 23 and 24, valve # 18 is opened carefully until the pressure in the sampling cylinder reaches about 1300 psig and liquid sample is taken. The valve # 18 is then quickly closed.

4. The valve # 25 is then opened slowly to collect the liquid sample in a clean sampling jar.

Shut Down

1. The electric power to the reactor heater is turned off.

2. The stirrer switch is turned off.

3. Hydrogen supply is cut off by closing the valves 11, 12, and 20.

4. The current to the temperature measuring and controlling instruments is turned off.

5. After 24 hours, the cooling water is cut off.

6. Before opening the reactor cover, the reactor is depressurized until the pressure of the reactor reaches an atmosphere.

APPENDIX C

CALCULATION PROCEDURE

After obtaining the weight percents of each compound in liquid samples, each weight percent was multiplied by the total amount of liquid in the reactor to give the weight of each compound left in the reactor. Obviously, the weight of oil in the reactor changed as samples were taken from the reactor. Therefore in every step, the mass of oil in the reactor was calculated by subtracting the sample mass from the previous mass of oil in the reactor.

The weight of each compound left in the reactor was divided by its molecular weight to obtain the total numbers of moles of the compound in the reactor. These are shown in columns marked "Mol of Quinoline" and "Mol of Py-THQ" in Tables VI, VII, and VIII. Experimental error in calculating the moles of quinoline and Py-THQ is discussed in Appendix D.

The conversion at reaction time t was calculated by using the following equation;

$$(Xa)_t = \frac{(\text{mols of Py-THQ})_t}{(\text{mols of quinoline})_t + (\text{mols of Py-THQ})_t} \qquad (A.1)$$

where $(Xa)_t$ is a conversion at time t.

Hydrogenation of quinoline to Py-THQ occurs both catalytically and non-catalytically. In order to evaluate the kinetics of catalytic reactions, in the analysis of conversion data, the contributions of noncatalytic reactions should be subtracted from the total conversion in the catalytic runs. Therefore, the amount of Py-THQ at time t produced by the catalytic reaction is calculated from the following formula ;

$$(\text{mole of Py-THQ})_t = (\text{mole of Py-THQ})_{t,cat.} - \frac{(\text{mole of Py-THQ})_{t,noncat.}}{(\text{mole of quinoline})_{t,noncat.}} * (\text{mole of quinoline})_{t,cat.} \qquad (A.2)$$

where

(mole of Py-THQ)t,noncat. = mole of Py-THQ at time t in noncatalytic reactions

(mole of quinoline)t,noncat. = mole of quinoline at time t in noncatalytic reactios

(mole of Py-THQ)t,cat. = mole of Py-THQ at time t in catalytic reactions

(mole of quinoline)t,cat. = mole of quinoline at time t in catalytic reactions.

APPENDIX D

REPRODUCIBILITY AND EXPERIMENTAL ERROR

The reproducibility of the system was evaluated by conducting run number 13, which is a duplicate of Run No. 1. The results of these two runs are plotted in Figure 24 and are given in Table XXV, which show the overall reproducibility of the experiments in terms of concentrations of quinoline and Py-THQ.

Any experimental measuring device will have certain uncertainities associated with it. Most of the uncertainities for the equipment have been determined through calibration or repeated analysis. The standard deviations in measuring the concentrations of liquid samples by GC were less than 0.048, as can be seen in Appendix A. The temperature probes were calibrated against a standard and was found to be within 1°C for the temperature range of this project. The pressure gauge was determined to have an accuracy of ± 20 psi. The accuracy of reading the weight of the liquid samples was estimated to be ± 1 mg. An example of the experimental error analysis is the calculation for the moles of quinoline and Py-THQ at time t. To calculate the number of moles, the total weight of the liquid mixture in the reactor must be known. The moles of a certain compound i at

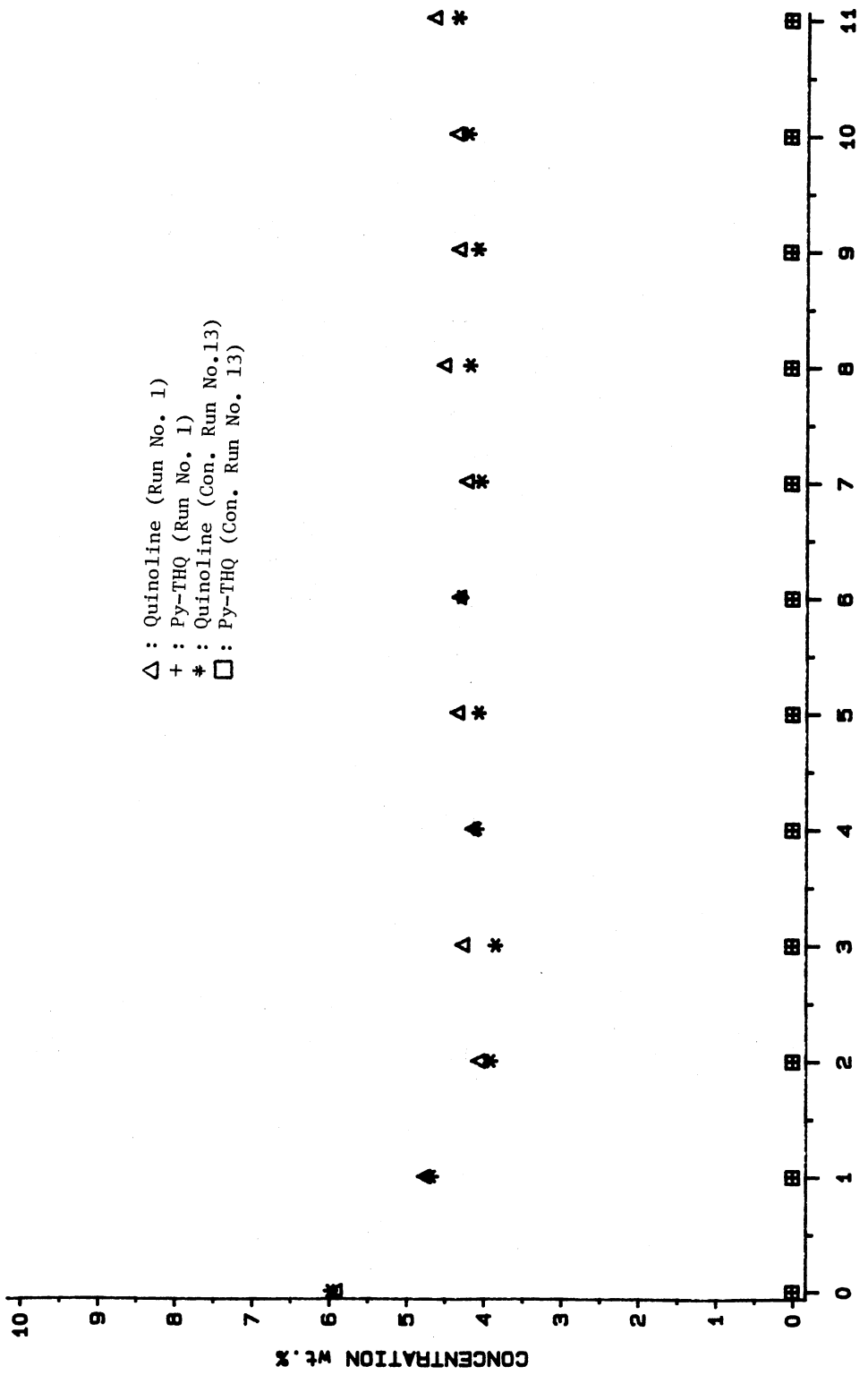

Figure 24. Reproducibility of the Concentrations of Quinoline and Py-THQ at 270 C (Run No. 1 and Con. Run No. 13)

TABLE XXV

REPRODUCIBILITY OF THE CONCENTRATION* OF QUINOLINE AT 270 °C (RUN NO. 1 AND CON. RUN NO. 13)

Run time (hr)	Run No. 1	Consecutive Run No. 13	Standard Deviation (%)
0	5.92	5.89	0.25
1	4.77	4.68	0.95
2	4.07	3.91	2.00
3	4.28	3.85	5.29
4	4.16	4.10	0.73
5	4.36	4.08	3.32
6	4.34	4.31	0.35
7	4.25	4.06	2.29
8	4.55	4.21	3.88
9	4.36	4.11	2.95
10	4.40	4.24	1.85
11	4.49	4.38	3.42
			2.48**

* Unit of concentration is wt.%
** Average of percent standard deviations

time t in the reactor is obtained as:

$$\text{moles of i} = \frac{\text{total weight of liquid mixture}}{\text{molecular weight of i}} * \text{wt.\% of i}$$

The cumulative error is then estimated as:

$$\sigma_t / \text{Mol}_i = [(\sigma_{tw} / tw)^2 + (\sigma_{wp} / wt)^2]^{1/2}$$

where σ_t is the cumulative error in calculating moles of i, σ_{tw} and σ_{wp} are the errors in calculating the total weight of liquid mixture and weight percent of i, respectively. Table XXVI shows the result of cumulative error analyses in calculating the moles of quinoline and Py-THQ, using the above equation.

TABLE XXVI

CUMULATIVE ERROR ANALYSIS IN CALCULATING MOLES OF QUINOLINE AND Py-THQ AT 330 °C (RUN No. 6)

Run time	Quinoline	Py-THQ
0	0.144 ± 0.0073	0
1	0.121 ± 0.0062	0.008 ± 0.0004
2	0.089 ± 0.0045	0.025 ± 0.0013
3	0.054 ± 0.0028	0.037 ± 0.0020
4	0.043 ± 0.0022	0.041 ± 0.0021
5	0.035 ± 0.0018	0.047 ± 0.0024
6	0.028 ± 0.0014	0.058 ± 0.0030
7	0.022 ± 0.0011	0.068 ± 0.0035
8	0.018 ± 0.0009	0.078 ± 0.0040
9	0.013 ± 0.0007	0.083 ± 0.0042
10	0.011 ± 0.0006	0.093 ± 0.0048
11	0.010 ± 0.0005	0.093 ± 0.0047
12	0.009 ± 0.0005	0.099 ± 0.0051

VITA

Byeong Il Noh

Candidate for the Degree of

Master of Science

Thesis: CATALYTIC PROPERTIES OF MOLYBDENUM NITRIDE IN HYDROGENATION OF QUINOLINE

Major Field: Chemical Engineering

Biographical:

Personal Data: Born in Kyungbuk, Korea, October 18, 1961, the son of Bum Ku and Chang Seon Noh.

Education: Graduated from Seoul Technical High School, Seoul, Korea, in January, 1980; received Bachelor of Science in Chemical Engineering from Hanyang University in February, 1984; completed requirements for the Master of Science degree at Oklahoma State University in December, 1988.

Professional Experience: Research Engineer in Daehan Electric Wire Ltd. (Seoul) in 1986; Graduate Teaching Assistant, Department of Chemical Engineering, Oklahoma State University 1987-1988.